STOCHASTIC RESPONSE OF TENSION LEG PLATFORM TO WAVE AND CURRENT FORCES

by

JUN-HEE LEE, B,S. in M.E.

A THESIS

IN

MECHANICAL ENGINEERING

Submitted to the Graduate Faculty
of Texas Tech University in
Partial Fulfillment of
the Requirements for
the Degree of

MASTER OF SCIENCE

IN

MECHANICAL ENGINEERING

May, 1988

ACKNOWLEDGMENTS

I would like to express my sincere appreciation to Dr. A. Ertas, committee chairman, for his guidance, continuous encouragement, support, and patience on this thesis. Also, I want to extend my gratitude to Dr. H. J. Carper and Dr. T. T. Maxwell for their time aind service as members of this thesis committee.

TABLE OF CONTENTS

ABSTRACT

The linear analysis in the frequency domain is presented for the surge motion of a tension leg platform (TLP) in the case of random waves only and random waves with constant current. A single-degree-of-freedom model of a TLP is employed for response, A simulation technique for determining the exact response statistics of nonlinear structural systems is developed in the time history. The superposition method, one of the simulation techniques, is applied to random sea wave with current, and the response analysis of TLP in time is developed with wave velocity and wave acceleration simulations.

Wave force is calculated using the modified Morison equation. The relative velocity due to the wave particle movement and the TLP movement is considered in both analyses. Current velocity that has a horizontal profile is applied for the model. The effect of wave-current interactions on the response analysis of TLP is examined.

Computational methods for both analyses are developed, and the results of stochastic, dynamic response of the TLP, with and without the presence of current, are discussed.

LIST OF TABLES

LIST OF FIGURES

NOMENCLATURE

o = spacing of corner columns in *x* direction

o' = effective length of hulls

6 = spacing of corner columns in *z* direction

h' = effective length of cross braces

c = structure damping coefficient

Cac = added mass coefficient for columns

CoH = added mass coefficient for hulls

Cx> = drag coefficient

Cm = inertia coefficient

DH = diameter of hulls

Di = diameter of *i* th columns

E = depth of center line of hull below M.W.L

⌈ = load per unit length on the structure

F = force on members

g = acceleration due to gravity

Gp ((jj) = transfer function of the wave loading

h = submerged depth

h(t) = impulse response function

H(<jj) = frequency response function

k = tether stiffness

K = wave number

LnL2 = linearization coefficients

Af., = added mass due to columns and hulls in x-direction
'•ax

Mp = structure mass

771, = structure and added mass in x-direction
„x

PF = probability function

PI = probability integral

r{t) = random relative velocity due to the water particle velocity and structure velocity

SFX(^) = spectral density of the wave loading

5„ *(u)* = power spectral density of wave amplitude

T = wave period

Uc = current velocity

Uw = horizontal wave particle velocity

$\dot{U}$^*r* = horizontal wave particle acceleration

X = lateral displacement of structure

$\dot{X}$ = structure velocity

$\ddot{X}$ = structure acceleration

p = density of the seawater

CE = standard deviation of wave velocity at depth E below MWL

GET = standard deviation of relative wave velocity at depth E below MWL

CTk« = standard deviation of wave velocity

c^r = standard deviation of relative wave velocity

CT, = standard deviation of structure response

(Pi = random phase angle uniformly distributed between 0 to 27r

rj{t) = wave amplitude

u; = wave frequency

u, = circular frequency of structure

CHAPTER I

INTRODUCTION

After the Industrial Revolution, the rapid growth of industry caused a change in major energy resources from coal to crude oil. The demand for petroleum resources has rapidly increased for the last two decades. Because of the limitation of natural resources on land, oil exploration was moved to shallow water areas, near the sea shore, which had the possibility of oil production. In shallow water fixed concrete and even wooden platforms were enough to support drilling and production equipment. As offshore oil exploration moved into deeper waters, steel frame structures and gravity concrete structures were developed. As the water depth and the severity of environmental loadings increased, the manufacturing and installation costs of fixed concrete or steel structures rose exponentially. Table 1-1 [l] shows the main characteristics of four offshore oil platforms. In the 1970s, with the discovery of the great oil fields in the North Sea, offshore structures had to be anchored on the sea bed 500 feet (152.4 m) below the water's surface and designed to withstand the impact of waves 100 feet (30.48 m) high.

Considerable interest has been focussed on a new class of structures, namely the compliant offshore structures. Tension Leg Platforms (TLP) are prominent new examples of this type. Tension leg platforms have as their principal characteristic a positively buoyant structure kept on location by a pretensioned anchoring system. The general schematic of a TLP

Table 1-1 Main characteristics of the four offshore oil platforms

	STATFJORD *B*	MAGNUS	HUTTON	BLOCK 280 (MISSISSIPPI CANYON)
LOCATION	NORTH SEA (NORWAY)	NORTH SEA (U.K.)	NORTH SEA (U.K.)	GULF OF MEXICO (U.S.)
STRUCTURE	CONCRETE GRAVITY	STEEL JACKET AND PILING	TENSION LEG	GUYED TOWER
TYPE	FIXED	FIXED	COMPLIANT	COMPLIANT
WATER DEPTH (FEET)	472	611	485	1.000
100-YEAR WAVE (FEET)	100	102	98	72
PRODUCTION (BARRELS PER DAY)	150.000	120.000	110.000	25.000
INITIAL PRODUCTION (YEAR)	1982	1983	1984	1984
MAXIMUM DECK OFFSET (FEET)	3	4	79	39
APPROXIMATE TOTAL COST (BILLIONS)	SI.8	S2.6	S1.3	$.8
COST PER BARREL-DAY	SI 2.000	$21,700	$11,800	$32,000
PROJECT MANAGEMENT	MOBIL	BRITISH PETROLEUM	CONOCO	EXXON

drilling and production system is shown in Figure 1-1. Tension leg platforms are connected to the sea bed by vertical steel tethers and riser. Tension leg platforms move with the waves rather than resist them. Hence, we call the TLP a compliant structure. Tension leg platforms offer the great promise for exploratory drilling, supporting production equipment in much deep sea. The dynamic characteristics of TLP's are substantially different from those of fixed offshore structures. Due to the corresponding stiffness of the mooring system for surge, sway, and yaw motions, the mean environmental forces (an average 15-second of longer natural period) are resisted by the mooring system and by the TLP inertia [2]. But under severe environmental conditions such as those in the North Sea, the horizontal displacement, or surge, becomes large. This large surge motion, which is a governing design parameter, creates high bending moments near the sea bed part of risers. Therefore, the design of a TLP for operation in severe sea conditions as in the North Sea requires reliable estimates for the expected maximum dynamic response of offshores structure due to environmental loadings.

Two fundamental approaches are available to determining the dynamic response of offshore structures due to wave action, two fundamental approaches are available. The first is the linear analysis in the steady-state frequency domain. The second is nonlinear dynamic analysis in the time domain. The frequency domain method is a closed-form solution requiring linearization of the dynamic equations of structure. This method assumes that all time dependent terms are harmonics, thus eliminating the time variables from

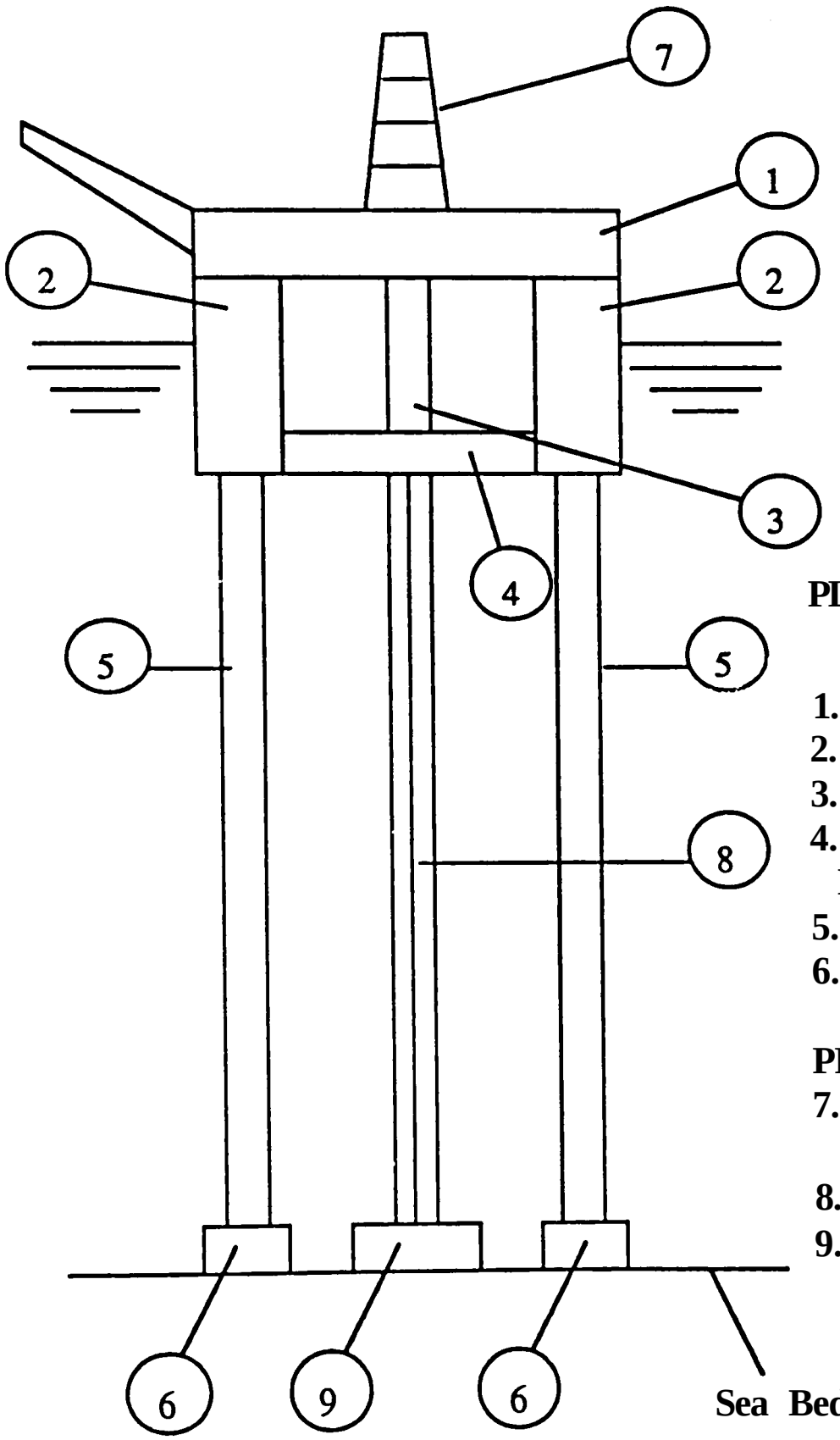

PLATFORM SYSTEMS

A) PLATFORM

1. **Deck**
2. **Corner columns**
3. **Cross braces**
4. **Hulls**

B) MOORING SYSTEM

5. **Tensioned steel tethers**
6. **Foundation templates**

PRODUCnON SYSTEMS

7. **Drilling and workover systems**
8. **Risers**
9. **Drilling template**

Figure 1-1 General TLP illustration

the equations. Since time is no longer an independent variable, there is no need to consider transient responses. Therefore, the frequency domain approach directly calculates the steady-state solution. The disadvantage of this method is that the nonlinear drag force term due to the relative velocity term in Morison's equation must be linearized. Since the nonlinear effects must be approximated by corresponding linear terms, the approximate, linearized terms of the nonlinear phenomenon have a low accurax:y compared to time domain analysis. Although time domain dynamic analysis, which analyzes numerically the nonlinear drag term on the relative velocity, is the most accurate, much more computation time is required. Statistical accumulation for a random wave C2ise requires much greater times compared to a regular wave case. Therefore, in this thesis, the frequency-domsdn method is adopted for the dynamic response of TLP's in random sea with a steady current.

The closed-form solution for the dynamic response of the TLP is derived and the numerical solution is also developed. The mathematical and numerical investigations consider the effects of the drag forces related to the random relative velocity between the TLP and the water particles, and the efllfects of the combined wave and current on the surge response of the TLP, The phenomenon of wave-current interactions which changes wave energy is examined for random waves with a steady current. For these purposes, a single-degree-of-freedom system for a TLP is employed. Wave-induced

forces are calculated using the modified Morison equation, which takes into account relative motion.

For comparison with the frequency-domain results, a time-domain simulation method for random sea waves with current is also developed. As new techniques for resolving the main disadvantage of the time-domain method, the amiount of computation time, are currently being developed and proposed, the chapter for the time simulation method is allocated to reviewing the recent developments of random time-domain simulation. Thus, Chapter VI shows the superposition method, one of the random time simulation methods. Numerical simulations are developed and the stochastic, dynamic response of the TLP is compared to frequency domain analysis.

CHAPTER n

LITERATURE SURVEY

2-1 Dynamic Analyses for Tension Leg Platform

Offshore structure behaviors sure either static or dynamic, but there is big difference between two analyses. For instance, in riser analysis for bending stress, static solution for maximum bending stress is close to sea surface, but dynamic solution for maximum bending stress is close to sea bottom as shown in Figure 2-1. Therefore, when the period of structure motion is more than two s, dynamic analysis must be utilized for structure motion.

Two fundamental approaches are used for the dynamic response of offshore structure:

1. Time history analysis
   a. Direct integration method
   b. Mode superposition method
2. Steady-state frequency domain analysis.

In the direct integration method, the equations of motion, which are function of time, are integrated using a numerical step-by-step procedure. A considerable amount of computational time is spent in the transient response as shown in Figure 2-1, which is generally of little interest. In the mode superposition method, the equations of motion are transformed into a modal space. A linear combination of mode shape is taken to be the dynamic response of offshore structure. Solution of the equations of motion in the modal space

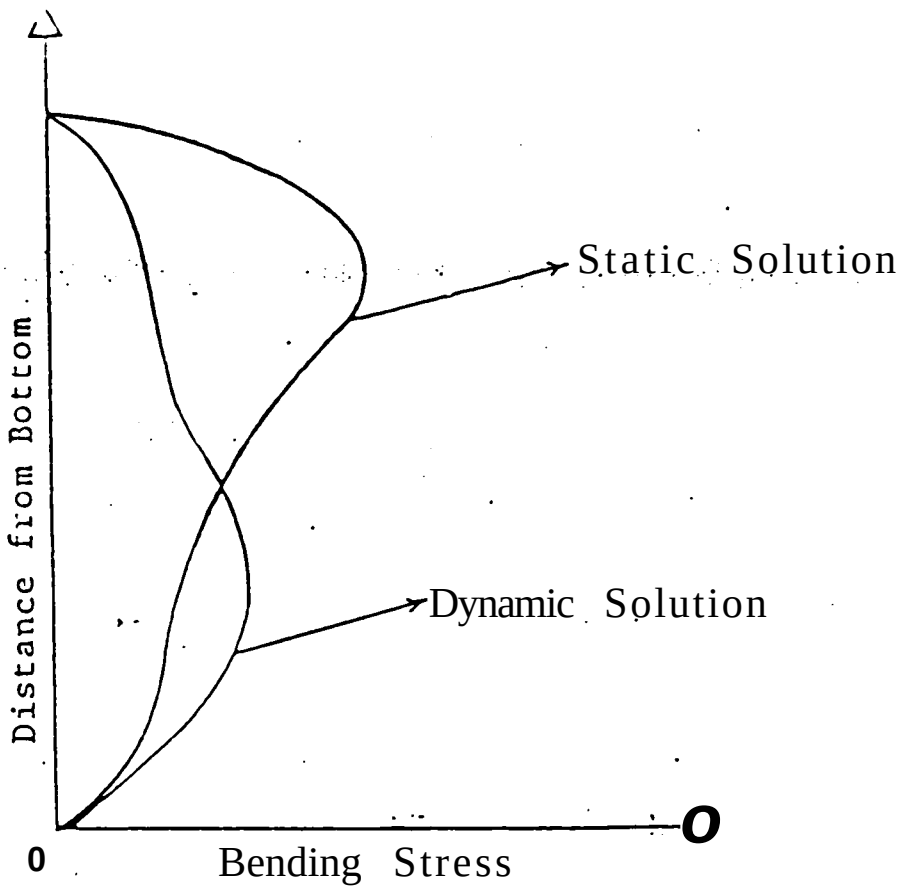

a) Static and dynamic solutions for maximum bending stress in riser

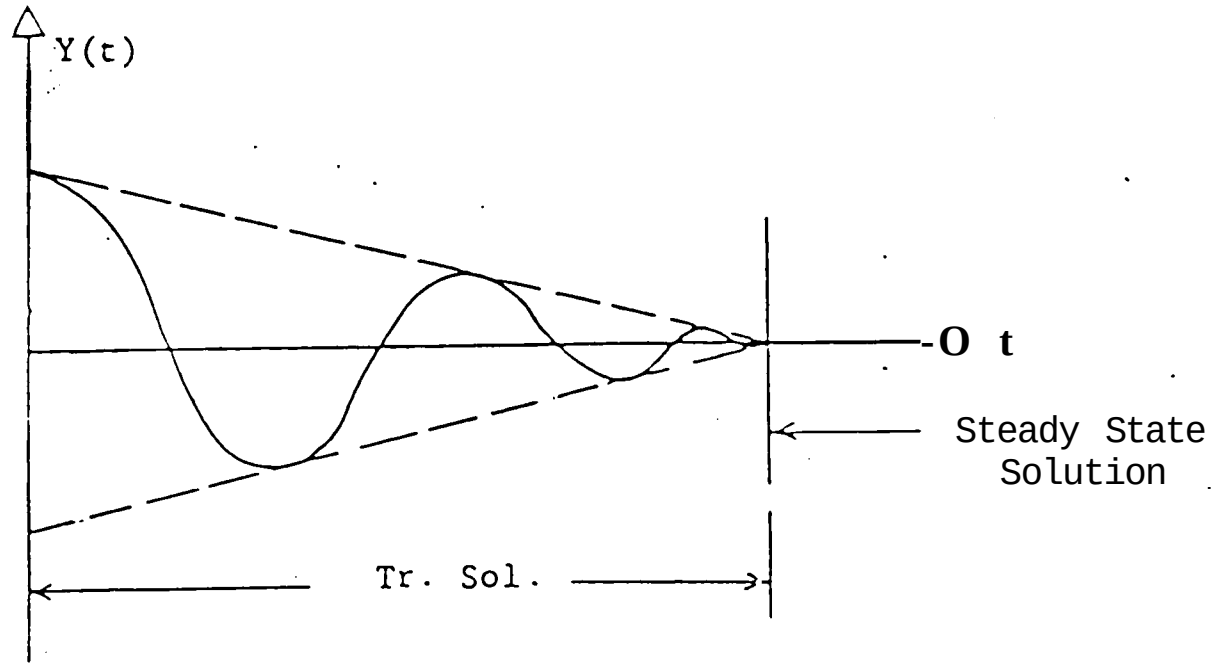

b) Transient and steady-state solutions of dynamic analysis

Figure 2-1 Static and dynamic analyses for offshore structures

takes a considerable saving in computational time. Generally, this method is faster and more economical than direct integration method. However, this technique also uses a considerable amount of computational time in obtaining the transient response.

In the steady-state frequency domain approach, it is assumed that all time dependent terms are harmonic, thus eliminating the time variable from the equations. Since time is no longer an independent variable, transient responses are not considered in frequency-domain analysis. Thus, the frequency-domain approach can directly calculate the steady-state solution.

The dynamic analysis mentioned in this section can be also applied to TLP, one of offshore structures. Considerable interest has developed in the use of compliant structures, thus, a number of papers have been published on the dynamic analysis of TLP's. Spanos and Agarwal [3] investigated the effect of wave forces calculated at the displaced position of compliant offshore structures on structural response. They used a single-degree-of-freedom structural model because of the mathematical complexities of system. Numerical integration procedures were used for solving a nonlinear equation of motion of structural response. They also developed approximate analytical solution techniques. For appropriate analytical solution, both deterministic ajid stochastic excitations were used.

Deleuil et al. [4] developed a new method for performing the dynamic analysis of offshore structure in the frequency domain. For a solution of the dynamic response of a structure in random seas, they used a second-Harder

spectral analysis. Numerical solutions of this relatively new method were developed, and the results of structure response were compared with those of a time-domain analysis.

Yoneya and Yoshida [5] investigated the dynamic responses of TLP's by several series of model tests in regular waves. Several simplified methods were also developed, and the responses of TLP's were verified by comparison with the test. Also, by using frequency-domain analysis, statistical calculations of TLP's for random response characteristics were performed for a real sea state.

Albrecht et al. [6] described the mathematical models for dynamic analysis of TLP's. The frequency-domain analysis and the time-domain analysis for the nonlinear equation of motion were considered. Particularly, the nonlinearities due to the tension cable were discussed.

Denise and Heaf [7] studied the importance of nonlinear effects by examining the dynamic behavior of TLP's due to wave action. Two mathematical analyses were presented for the hydrodynamic characteristics of the structure. The first was a linear diffraction-radiation theory for the linear response, and the second was a three-dimensional, time-domain simulation for the nonlinear motion response. Both methods were used to predict the dynamic responses of TLP's and the tensions in the mooring lines.

Oran [8] treated the TLP as a continuous mechanical system with a number of free vibration modes and frequencies. The variations in the dynamic response characteristics of a TLP were evaluated as a function of the water

depth. The important parameters, such as the tether/platform weight ratio, the period of the "principal modes," and the periods of the "secondary modes," were considered.

Ninomiya et al. [9] proposed an approximate response analysis method for TLP's in very high waves by using the finite amplitude and nonlinearized theory. The analytical results of this method were compared with the results of systematic tank tests for applicability to practical problems. A computer simulation was conducted on a prototype model of a TLP with and without a mechanical damping system for verifying the nonlinear response characteristics of TLP's in very high waves. Applicability of the models to practical problems was also discussed. An in-laboratory dynamic loading test was performed to verify the performance of the hydraulic damper.

Finnigan et al. [10] presented and evaluated the experimental time-domain model test for the prediction surge response of a TLP in regular and random waves in the presence of a current. Its primary purpose was to verify the final design. A secondary purpose was the development of response amplitude operators (RAO's) for frequency-domain analysis procedures.

Botelbo et al. [11] presented and evaluated a frequency-domain method for predicting the extreme surge response of TLP's in random waves with a current. The surge motion of a TLP critically influenced the design of tension cables and risers.

Yoshida et al. [12] developed a linear response analysis method of TLP's under regular waves. This method analyzed response motions, tension variation of tethers, and structural member forces. The applicability of this method was verified by compauring with the results of TLP model tests.

In extremely deep water, rolling, pitching, and heaving motions of the structure have a significant effect, which results in the elongation of the tensioned cables. Elasticity of mooring cables is a very important factor in field operations, thus, Yashima [13] evaluated this property with tank tests. The theoretical model was developed, and the results were compared to the experimental results.

Paulling and Horton [14] presented a linearized hydrodynamic synthesis technique for the prediction of structural motions and tension forces because accurate predictions of platform motions and tensioned forces are important design factors in the reliability of the anchoring system. Model experiments were performed for comparison with the theoretical results,

Sekia and Sakai [15] conducted hydrodynamic model tests to establish a design method of TLP-tether systems. Also, analytical solutions using linearized and nonlinear methods were performed on TLP behavior. The analytical results were compared with the model test results; this indicated that the linearized analytical method could accurately predict the response of TLP.

Jefferys and Patel [16] described models of the tether lateral oscillation dynamics for the prediction of lateral resonant frequencies and amplitudes

in the wave frequency range on the motion of a TLP, A Mathieu type of unstability in the TLP sway motion due to the tension change in time was investigated using *am* energy balance approach. Nonlinear square law damping was shown to place an upper bound on oscillation amplitude,

Angelides et al, [17] considered the influence of TLP hull geometry, values for force coefficients, water depth, pretension, and tether axial stiffness on the dynamic response of TLP's in extreme sea states, A six-degree-of-freedom model was used for the response analysis of the floating body.

Kirk and Jain [18] studied the dynamic response analysis of a tension-leg single buoy mooring system due to regular waves. Swaying motion, which caused the stretching of the tension cables and the pitching motion that created slack in the anchor cables, was considered in the nonlinear equation of motion. The dynamic pressure force acting on the base of the buoyed structure was also included in the mathematical model, A numerical solution was developed to predict the response of offshore structures. For the applicability of realistic wave time histories, a deterministic method analyzing the nonlinear equations of motion was used.

2-2 Linearization Techniques for Offshore Structures

The drag force, which is proportional to the square of the relative velocity between the wave particles and the structure, creates the nonlinearity in the equation of motion. The drag force term with nonlinearity must be

linearized for the steady-state frequency domain approach. The numerical computations of the frequency domain analysis with linearization techniques are much faster than those of the time domain analysis. However, this method has less accuracy caused by the linearization coefficients. Therefore, it is very important to choose the proper linearization technique. Many researchers have proposed linearization techniques that apply to the nonlinear hydrodynamic drag force,

Krolikowski and Gay [19] developed a new, improved linearization technique for frequency domain analysis where the hydrodynamic drag force was linearized. This technique was applied to risers under regular and random waves with and without current. Riser responses were calculated with this method and were compared with responses obtained from a transient solution of time-dornain analysis. The frequency-domain solution with the new linearized drag force showed good accuracy compared with the nonlinear time domain especially for regular waves.

Ertas and Kozik [20] presented the principles of riser modeling and numerical approaches for performing dynamic analysis of a marine riser. The linearization technique for the dynamic response of a marine riser was given. The linearization technique was applied to cases of regular waves with and without current. The authors recommended the frequency domain approach for marine riser analysis, especially for regular waves and regular waves with low current velocity (up to 0,7 knot).

Ertas [21] described linearization coefficients for the nonlinear drag effect, which took into account random waves and current. The derived linearization coefficients were in agreement with the linearization coefficients derived by Krolikowski and Gay [19], This technique can be directly applied to analyze the dynamic response of marine risers. The describing function method was used to determine the linearization coefficients for the nonlinear hydrodynamic drag forces, taking into account a steady current and the random sea waves.

Bernitsas [22-24] developed a comprehensive nonlinear model for the dynamic response of a marine riser. Large three-dimensional lateral oscillations were modeled in the local principal osculating and rectifying planes. Also, longitudinal extensional oscillations were considered in the local tangential direction. Bernitsas also presented the significance of three-dimensional bending effects and the contribution of the nonlinear terms.

Leira and Olufsen [25] proposed a method to multiplanar excitation and three-dimensional response of offshore structure. The minimum mean square error (MMSE) stochastic linearization method was developed, a restricted MMSE method was applied to marine riser analysis, and the results of this technique were compared with those of the simplified linearization method.

Wu and Ray [26] studied the stochastic dynamic response of offshore structures with and without current. Since the drag force has the nonlinear term related to the fluid particle velocity, it cannot be regarded *as* a simple superposition of current and wave drag forces. Therefore, the authors

developed the equivalent linearization technique to allow the use of the normal mode superposition method for solving the nonlinear, stochastic differential equations of structural responses due to combined actions of current and waves. They also developed a computer program for the practical application of their analytical approach and showed the importance of including currents in the dynamic analysis.

Berge and Penzien [27], Foster [28], Langley and Kirk [29], Langley [30], Malhotra and Penzien [31], Sigbjornsson and Smith [32], Spanos [33], and Young et al, [34] have studied one-dimensional and multi-dimensional random dynamic analysis of offshore structures using the linearization technique. Although the linearization techniques mentioned here usually have been applied to risers, these techniques also can be applied to the TLP model.

CHAPTER HI

BACKGROUND

3-1 Introduction

The primary purpose of this chapter is to show the oceanographic information needed to analyze the dynamic response of offshore structure in the sea. The major environmental loadings such as waves and currents were introduced.

To evaluate the fluid-induced forces acting on an offshore structure, it is necessary to know several environmental factors, such as winds, currents, and surface gravity waves. Although real ocean phenomena always occur in various combinations, the scope of this thesis is limited to currents and surface gravity waves. Therefore, this chapter shows an overview of ocean waves and currents. Waves generate dynamic loads; ocean currents generate static loads. For a more detailed information, the reader is referred to references [35], [36], [37], and [38].

3-2 Waves

Although deterministic approaches are useful for describing the short term features of ocean waves, probabilistic approaches are more useful in describing the long term features of ocean waves for structural fatigue. To describe the characteristics of irregular waves in a statistical manner, it is necessary to know the field record of real, irregular ocean waves. Ocean waves

can be represented by their energy spectra which are the important information for studying probabilistic analysis.

3-2-1 Wave Generation

Waves, which directly generate the loading to offshore structure, are primarily caused by the wind. Those waves directly generate the loading to offshore structures. When two adjacent layers of sea water and wind move at different velocities, a flow instability due to different frictional stresses occurs at the air-water interface. A light wind of only two knots or less causes small ripples on the sea surface. As the wind speed increases for any duration, the wave height builds up, and larger "gravity waves" begin to develop. Therefore, a more complex pressure distribution at the sea surface acts on the surface profile to further wave development. Although the exact way the growth of wind waves begins is not completely understood, there are many semi-empirical relationships that describe the growth of wind waves reasonably well.

The growth of wind waves is primarily based on three parameters: the fetch length F or the distance over which the wind blows, the wind velocity C', and the duration of time for which the wind blows. If a steady wind speed is given, the development of waves may be limited by the fetch length, or the duration time. However, if the wind blows over a sufficient distance for a sufficient time, a steady state condition, where the average wave heights

do not change, will occur. This condition is called a fully-developed wind sea, which is basic to wave forecasting.

3-2-2 Wave Statistics and Wave Spectrum

Any detailed analysis of the sea state requires the record of actual wave measured in ocean sea because of the random nature of waves. The examination of wave records by numerous researchers shows that the probability of the occurrence of a given wave height roughly follows the Rayleigh distribution. This is shown schematically in Figure 3-1 [36].

The arithmetic average of the highest one-third of the wave heights in a wave record is defined as the significant wave height H_s, which corresponds well to wave height estimates reported from visual observations. Therefore, the concept of a significant wave height is basic to the foreccisting and observation of ocean sea waves. If the significant wave height is known, other statistical parameters can be obtained from statistical probability distributions. The significant period T_s, which is associated with a significant wave height, is also the average period of the highest one-third of the waves in a wave record.

The movement of the wave form corresponds to the transmission of energy. The elevation of the irregular sea surface at any point in time at a given location will follow the normal, or Gaussian probability distribution. The total wave energy, composed of kinetic energy due to the orbital motion of the water particles and potential energy due to the difference in elevation

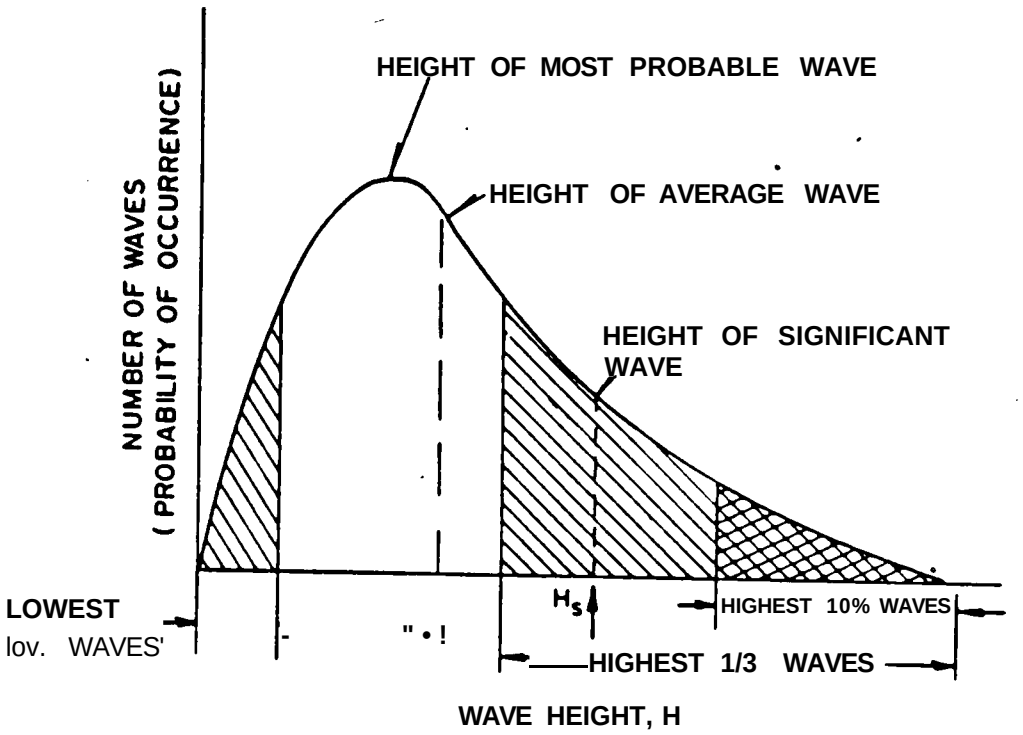

Figure 3-1 Rayleigh probability distribution of wave height

(trough to crest) of the particles, is proportional to the square of the wave height. The sum of the squares of the component heights or amplitudes is related to the energy spectrum of the wave system. Therefore, the wave energy spectrum indicates the amount of energy in the infinite number of component waves that yield the irregular sea pattern.

3-3 Wave Energy Spectra

Some of the well-known, one-dimensional frequency wave spectra that have been employed to describe ocean waves are introduced here. Many of these were developed in terms of a reference wind speed *U*. Bretschneider [35] and Pierson-Moskowitz [35] spectra are perhaps the most commonly used. The JONSWAP [35] spectrum, which is an extension of the Pierson-Moskowitz spectrum to take into account the higher peaks of spectra, is more recent and involves additional parameters. Wave energy spectra are derived from records of actual waves measured in generally similar sites and environments.

3-3-1 Darbyshire Spectrum [35] (1952)

This spectrum was one of the earliest to be used and is given as

$$S(f) = \begin{cases} 1.169 \times 10^{-}{}^{C}/^{*}\exp[-10.79(f - f_o)/(f - f_o + 0.0422)^{]} & \text{for } f - f_o > -0.0422 \\ 0 & \text{otherwise} \end{cases} \qquad (3\text{-}1)$$

where

U = wind speed *(m/s)*

/= circular frequency *(Hz)*

fo= 1/(1.94C/^ -h2.5 X 10-^C7^) : peak frequency.

This spectrum can apply to fully-developed sea conditions, hence, only the wind speed *U* is required.

3-3-2 Neuman Spectrum [35] (1953)

This spectrum is given as

$$S(f) = 2 \text{ X } 10\text{-}^{\wedge} gf\text{-}^{\wedge} \exp\left[\frac{B}{f^2}\right] \qquad (3\text{-}2)$$

where

$$B = \frac{g^2}{2ir^{\wedge}U^{\wedge}},$$

The peak frequency /o can be written as

$$f_0 = \frac{g}{\sqrt{6}\pi U} = \left(\frac{iB^{\wedge}x}{3}\right)^{\frac{1}{2}}.$$

This spectrum also requires wind speed *U* and so relates to fully-developed sea conditions.

3-3-3 Bretschneider Spectrum (1959)

This spectrum is given in terms of the significant wave height *H,* and peak frequency /o rather than the wind speed. The significant wave height *H,* and peak frequency /o are first obtained from relations in terms of the wind speed (7, the fetch length F, and the duration time *t.* Therefore, this spectrum applies to developing seas and is written as

$$5(/) = {}^{\wedge}ir,V_{\text{„}}\text{-}'(///_{\text{„}})\text{-}'\exp\left[\frac{-5}{4}(i\text{-})\text{-}\right] \qquad (3\text{-}3)$$

The Bretschneider spectrum is designed to ensure that the area under the spectrum curve corresponds to *H,/l6,* as should be the case on the assumption of a Rayleigh distribution of wave heights.

3-3-4 Pierson-Moskowitz Spectrum (1964)

This spectrum is given as

$$S\{f) = ag'(27r)-*r'exp[-0.74(:^rr'] \qquad (3-4)$$

where

a = 8,1 X 10" ® and is called the Phillips' constant.

This spectrum was developed semi-empiric ally by the analysis of extensive wave data relating to fully-developed sea conditions in the North Sea. Since the lower frequency is present, the Pierson-Moskowitz spectrum is applicable only for fully-developed sea conditions [39].

3-3-5 JONSWAP Spectrum (1967)

The major goals of the Joint North Sea Wave Project (JONSWAP) were to measure the growth of waves under a fetch-limited sea and to account for much sharper peaks of spectra in a storm condition for the same total energy as compared with the Pierson-Moskowitz spectrum [40, 41], The JONSWAP spectral density, which is widely used for representing fetch-limited seas, is given by

$$S,(/) = aff^(2^)-Vexp[-^(^)^]$$
$$xy-p[-(/-/.-)'/(2-'/i)] \qquad (3\_5)$$

where

a= scale parameter

g= gravity acceleration

/= frequency *(Hz)*

fm = peak frequency *(Hz)*

7= peak shape parameter, which is the ratio of the peak spectral energy to that of the corresponding Pierson-Moskowitz spectrum for the same *a* and /„„ values

(7 = *(Ta forf* ≺ *fm*

o= *Cbforf* > *fm*

Ga = left side width

(7b = right side width ,

The JONSWAP spectral formula has five parameters: 7, *fm,* a, and *da* and *at,* for *f* ≺ *fm* and *f* > *fmy* respectively. From an analysis of measured data, Hasselman et al, [40] provide the following average values for each parameter, and the resulting spectrum is called the mean JONSWAP wave spectrum.

a= 0.076(F)-°"

F= *gF/U*^

fm= *fm9/U*

fm= *3.5(F)-''''*

7 = 3.3

(7a= 0.07

cIb= 0.09

3-3-6 Modified JONSWAP Spectrum

For analyzing the response of offshore structures in fetch-limited waters, it has been customary to apply the JONSWAP spectrum, defined by the wind speed *U* and the fetch length F, as shown in Equation (3-5), However, for simplicity as well as for compatibility with the current technique in performing the offshore structure's operation, a JONSWAP expression that depends only on two parameters, namely the significant wave height *H,* and the modal wave period *Tm* can be derived.

Lee and Bales [42] have rewritten the JONSWAP equation in terms of significant wave height and period rather than wind speed and fetch length as

$$SM) = \wedge\wedge J \wedge \S \wedge s M 2, r) - V - = \text{«xp}[-1.25(/r_{\text{„}})-]$$

$$X7\ \text{e«p}[-(/r_{\text{„}}-i)V(2\text{«}T')], \qquad (3-6)$$

By simply converting / to w, the circular frequency in rad/s. Equation (3-6) can be further modified as

$$S_\eta(\omega) = \frac{16.942 H_s^{1.375}}{g^{1.375} T_m^{2.75}} g^2 \omega^{-5} exp\left[-1.25\left(\frac{\omega}{2\pi} T_m\right)^{-4}\right]$$

$$X7\ \exp[-(wT_{\text{„}}/(2,r)-l)V(2\text{«}T')] \qquad (3-7)$$

where

$7 = 3.3$

$a = 0.07$ for $\wedge \leq 5\wedge$

or

$$a = 0.09 \; ioT \; f\text{->} \; :\hat{} \; .$$

This modified JONSWAP spectrum will be applied to the dynamic analysis of the tension leg platform model in this thesis; an example is shown in Figure 3-2.

3-4 Selection of Design Wave Spectrum

All the proceeding wave spectra are best-fit curves of a number of individual spectra, each derived from records of actual waves that are measured in generally similar sites and environments.

The wave spectra selected for evaluating the design of a particular structure depends on several factors. One of them is the risk criteria adopted by the owner of the structure. The owner must decide what risk can be economically justified for a particular structure located at a given site. For instance, the most economical overall design may be based on a storm occurring on the average once in 20 years or once in 100 years.

Because wave spectra are derived from measured recordings at a site, the reader is encouraged to consult the most recent references concerning wave spectra. Thus the most up-to-date data are used to generate the family of design spectra. Once these spectra are determined, they can be applied to random dynamic analysis of offshore structural design.

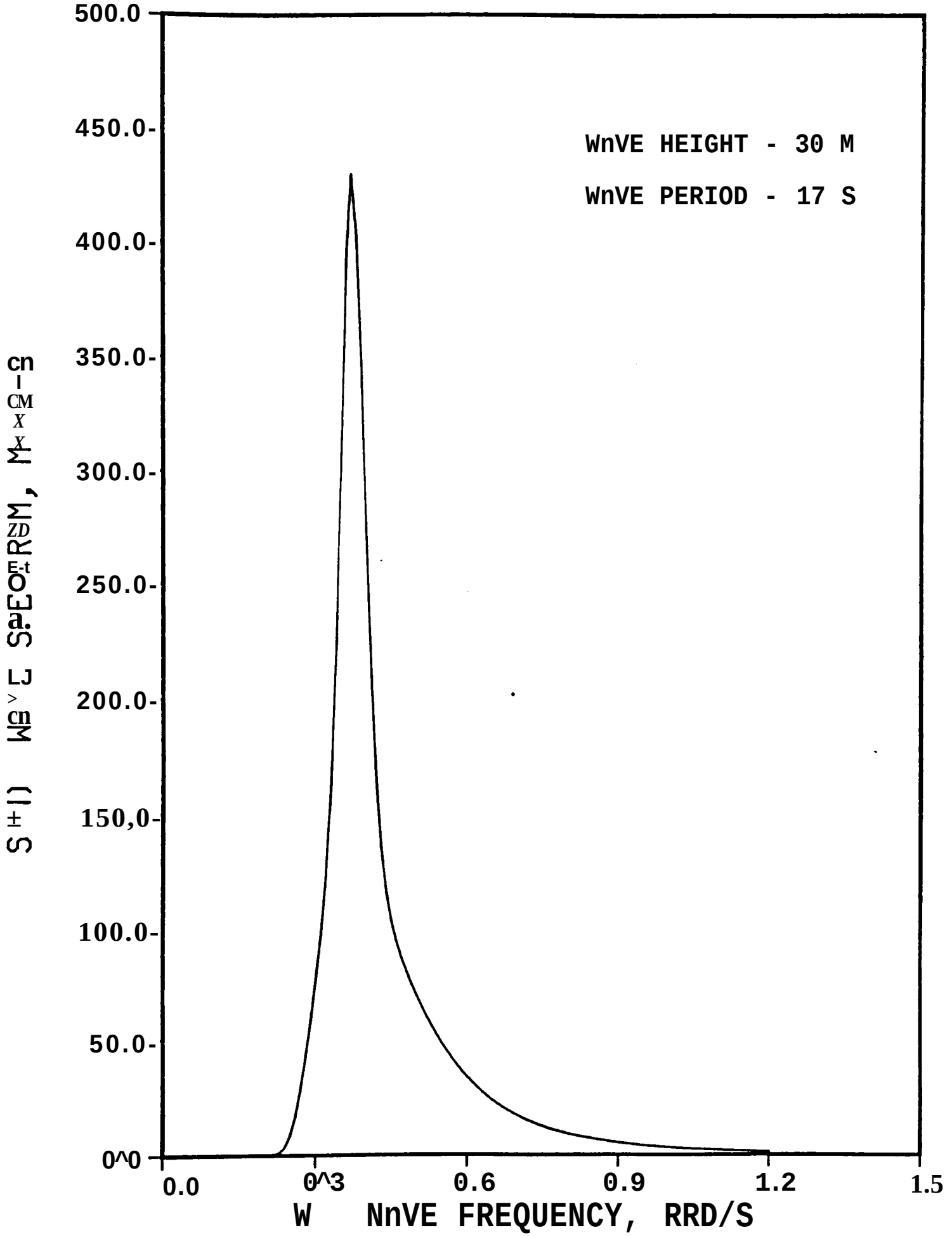

Figure 3-2 Modified JONSWAP wave spectrum with 101 wave frequencies

3-5 Current Effects

Currents are usually regarded as a horizontal velocity profile that decays very slowly with depth. The most common currents considered in offshore structural design are tidal currents.

Currents are another major source of environmental loading on offshore structures. The current has its main effect in force calculations. Because the drag force on a structural member is proportional to the square of fluid particle velocities, a small current may have a significant effect, particularly in a deep sea. The total fluid particle velocity is considered as the vector sum of current velocity and wave particle velocity. Since the drag force has a nonlinearity related to fluid particle velocity, it cannot be regarded as a simple superposition of current and wave drag forces in the dynamic analysis of offshore structures.

Longuet-Higgins and Stewart [43] studied the phenomenon of wave-current interactions for the case of a single wave. They showed that for a single wave, when the current is in the direction of the wave, the wave length increases and the wave amplitude decreases. When the current opposes the wave direction, the wave length decreases, but the wave amplitude increases. In a random wave field, Huang, et al. [44] and Tung and Huang [45] suggested that component waves are affected by current in a similar manner resulting in the modification of the wave spectrum as

$$\wedge nc(i\wedge) = \frac{45_{\prime\prime}(cj)}{[i + (i+4C/cu;/y)\wedge/1[(l + 4C/cu;/\wedge)\wedge/2\text{-}h(l + 4t/ca;/\wedge)]} \quad \wedge\wedge \text{ " } \wedge\wedge$$

where

Uc = current velocity *(mis)*

5„ = wave spectrum without the influence of current,

The current velocity *Uc* is considered to be steady in time and uniformly distributed in depth, Wu and Ray [26] developed a formulation to determine the stochastic, dynamic responses of offshore platforms with proper consideration of the nonlinear effect due to the combined actions of currents and waves.

CHAPTER rV

MATHEMATICAL MODELING

4-1 Introduction

Environmental loadings on a typical offshore structure include waves, currents and wind as shown in Figure 4-1. In deep water, hydrodynamic forces due to wind are less important than the sea induced forces. Therefore, this research will concentrate on fluid loadings due to current and waves. The wave kinematics are based on the linear wave theory. Current has a linear or bilinear velocity profile that varies with the depth of the water. The wave and current motion and the structure motion are assumed to occur in the same plane. Hydrodynamic drag forces generally have a very strong influence on the dynamic analysis of offshore structures, and they create the nonlinearity in the governing differential equation of motion. The dynamic responses for the surge motion of TLP's in the frequency domain are derived in the following sections.

4-2 Simplifications and Assumptions

The mathematical model derived in this research is based on the following simplifications and assumptions:

1. The structure is rigid as a whole.
2. The linear wave theory is adopted for wave particle velocity and acceleration.

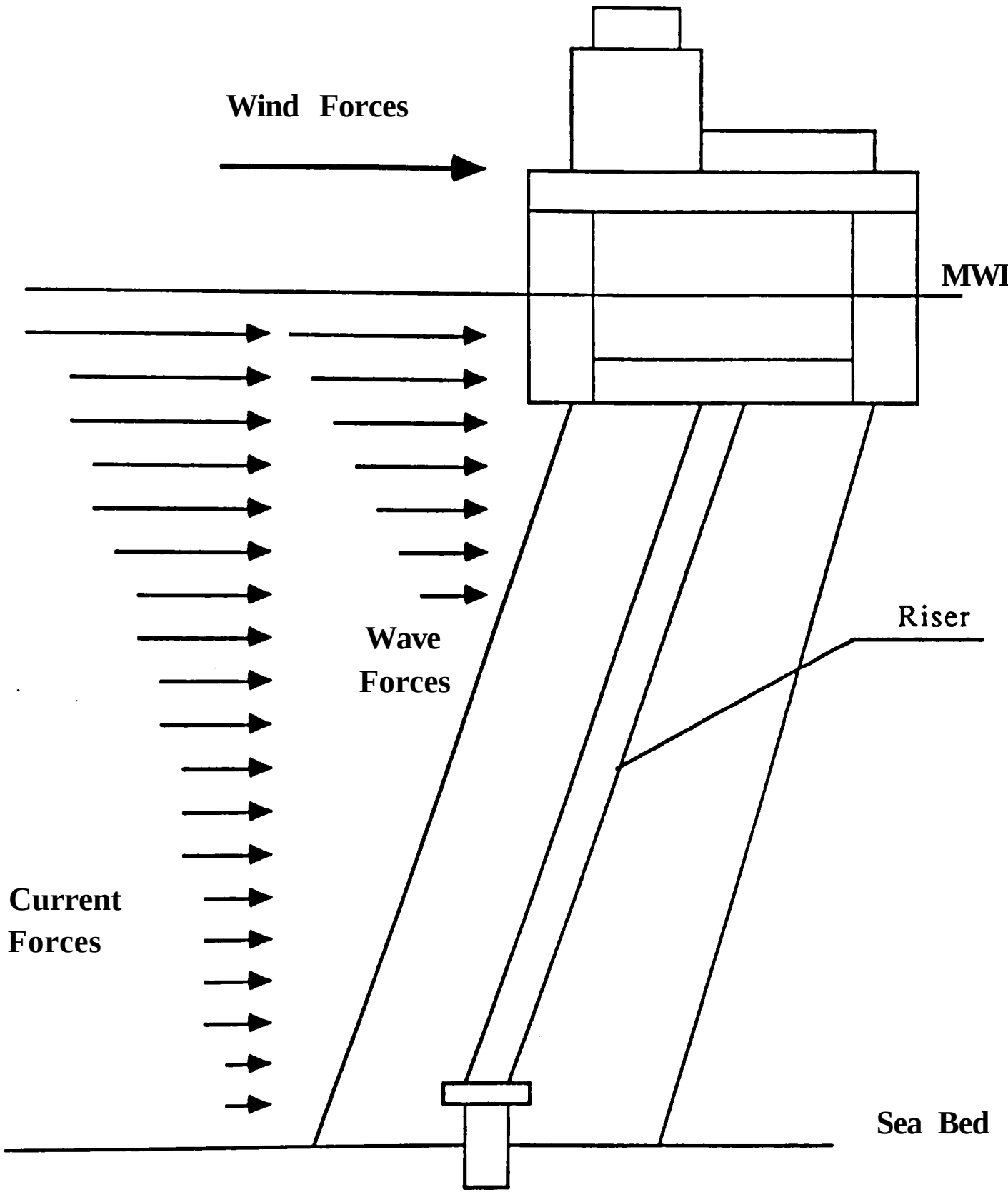

Figure 4-1 Environmental loadings on TLP

3. The effects of wave diffraction and sheltering for wave forces are neglected.
4. Hydrodynamical interaction between the neighboring hull elements is neglected,
5. Hydrodynamic forces on connecting members and mooring legs are neglected.
6. By using the root mean square (r.m.s.), wave induced drag forces in Morison's equation are linearized,
7. Pre-tension in the anchoring tethers remains constant, and every tether is subjected to pre-tension sufficient not to slacken.
8. Integration of wave forces on the submerged columns is carried out from the mean water level to the bottom of columns.
9. Gravity force, inertia force, hydrostatic forces, and hydrodynamic forces applying to tethers are neglected. Only the axial forces acting on tethers are applied to the structure as mooring forces.
10. The wave, current, and structure motions are taken to occur in the same plane.
11. The current is in the direction of the waves.
12. Hydrodynamic force involves only the horizontal components of the current velocity and the wave particle velocities.
13. The hydrodynamic damping term in the equation of motion is neglected.
14. The surge motion of the structure is considered.

4-3 Mathematical Formulation

A TLP model with four vertical columns, four horizontal hulls, and bracing members is adopted for mathematical formulation, with the surge motion of the TLP being the main consideration. The model is shown in Figure 4-2, All forces are considered as acting on the center of mass of the structure under the assumption that the structure is rigid *ajs* a whole. The response of the TLP in the *x* direction, the surge motion, is given by the solution of the following differential equation as a single-degree-of-freedom oscillator driven by environmental loadings:

$$m\ddot{x} + cx + kx = f(xyt) \qquad (4-1)$$

where

m, = structure and added mass in the *x* direction

$\dot{c}$ = structure damping coefficient

k= *X* component of tether stiffness.

The hydrodynamic force, *f(x,t),* on the structure can be found by separately computing the inertia and drag force related terms. In this research, the wave force was calculated from the modified Morison equation. Including the current velocity, the force / per unit length of a member of diameter *D* in the *X* direction at depth *y* can be written as

$$\bar{f}(x,t) = \bar{f}_D + \bar{f}_I$$

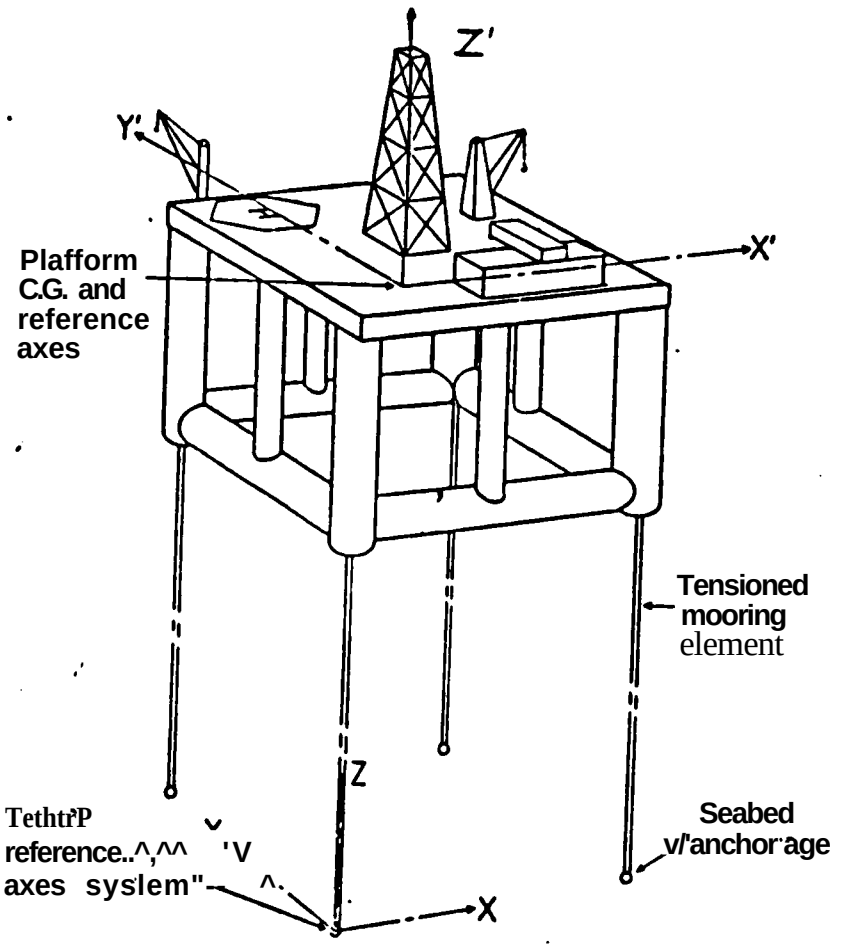

a) TLP structure and basic notation [16]

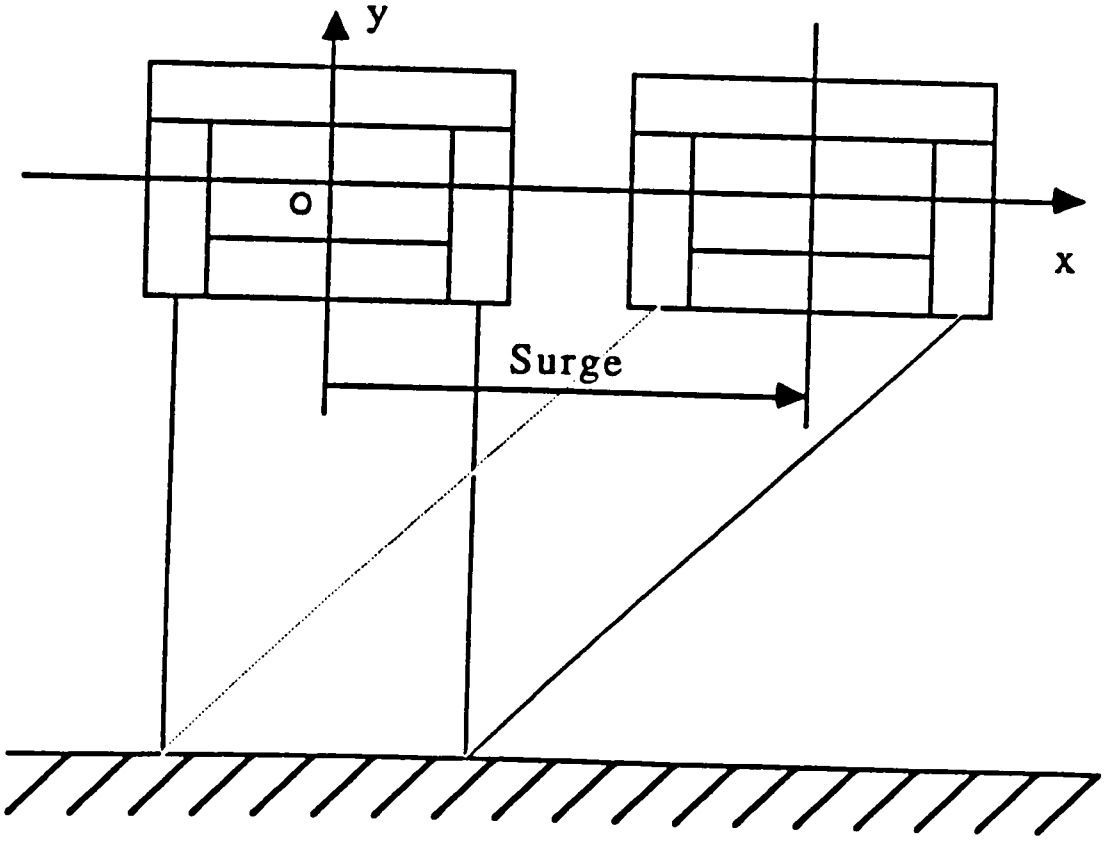

b) System schematic for surge motion

Figure 4-2 TLP schematic

or

$$f(x,t) = \frac{1}{2}\rho D C_D \{U_w + U_a - \frac{dx}{dt}\}\left|U_w + U_a - \frac{dx}{dt}\right| + \rho C_m \dot{U}_w + \rho I (C_m - 1)\{\dot{U}_w - \ddot{x}\} \quad (4-2)$$

where

ρ = density of sea water

C_m = inertia coefficient

C_D = drag coefficient

U_w = wave particle velocity

$\dot{U}_w$ = wave particle acceleration

U_c = current velocity

dx/dt = structural velocity

d^2x/dt^2 = structural acceleration,

The drag force term must be linearized before application in the frequency-domain analysis procedures.

4-4 Linearization Method

Although the linearization technique originated more than a century ago, it has gained special significance in recent years because of the requirements of the theory of oscillations. The early theory of linearization technique was developed by Krylov and N. Bogoliubov[46].

A system whose performance obeys the principle of superposition is defined as a linear system. If the superposition does not hold, then the system

is nonlinear. Nonlinear systems must be dealt with, because they occupy very important places in practical systems. When inputs are limited, linear approximation to nonlinear real systems gives very good results. However, most physical variables, if allowed to take on large inputs, will eventually run out of their range of reasonable linear approximation.

There are many linearization techniques that can be applied for different types of nonlinear systems. In this thesis, the describing function method derived from control theory will be applied to find the linearization coefficients [47, 48]. The describing function method (or method of harmonic balance) is a means of finding approximations to periodic solutions of nonlinear, ordinary, differential equations by replacing the nonlinear terms with a linear representation of their effect on a single harmonic. The describing function method is a form of quasilinearization that minimizes the mean squared error between the output of the original nonlinearity and the linear replacement.

In the describing function method, the concern is basically the frequency response of the system. If x is the input to a nonlinear element, the input-output relationship is given as

$$Y(t)=Y[X\{t),\dot{X}(t)] \qquad (4-3)$$

where

Y= nonlinear function of sinusoidal input X.

The output will have the same frequency as X plus components of higher harmonics. Since the fundamental frequency is dominant, higher order harmonics can be ignored.

The linearization is dependent on the form of the input to the nonlinearity. In this thesis, for the tension leg platform, two kinds of input describing functions will be discussed:

(a) Random-input describing function, used for random wave cases.

(b) Dual-input (random plus bias) describing function, used for random wave with current cases,

A number of papers mentioned in section 2-2 of Chapter II shows one-dimensional or multi-dimensional random dynamic analysis of offshore structures in frequency domain. In these studies it has been shown that frequency-domain approaches for dynamic structural analysis, using approximate linearization techniques, result in a great decrease in computational time (about two orders of magnitude less) when compared with time history analysis and yet yield accurate results.

The combination of the hydrodynamic forces exerted on the cylindrical structures per unit length is given by Equation (4-2). The first term in Equation (4-2), called the drag term, needs to be linearized. For TLP application, a linearized version of the nonlinear drag term for steady-state current (constant input) and random waves can be formulated as

$$FD = \backslash PDCD \text{ La } Uc + \backslash pDCo\ L, r(t) \qquad (4 - 4)$$

where

L1, 1/2 = linearization coefficients.

The linearization coefficients need to be determined so the mean-square approximation error is minimized; they are given as follows:

CASE 1 : Random Wave Only

$$Z. = V f 2a \qquad (4\text{-}5)$$

$$La = 0$$

CASE 2 : Random Wave with Current

$$Ll = 4GPF(\wedge) + 2Uc\,[2P/(\frac{U_c}{\sigma}) - 1] \qquad (4 - 6)$$

$$L. = 2GPF(\wedge) + C7C\,[1 + (\wedge)\wedge]\,[2P/(\wedge) - 1] \qquad (4 - 7)$$

where

PF= **probability function**

PI= **probability integral**

G= **standard deviation of the unbiased stationary random process .**

The unbiased stationary Gaussian random process, r(t), can be normalized with respect to the standard deviation *G* as

$$v = \frac{I}{G}$$

and probability function is given by

$$PF(V) = -\wedge \underset{v/27r}{} exp(-\wedge) \qquad (4\text{-}8)$$

Probability integral can be written

$$PI(V) = -\wedge f\_\wedge\ exp(\sim)dV\wedge \qquad (4\text{-}9)$$

The probability integral can be written in terms of the probability function as the following (Gelp and Vander [48]):

$$-\int V\text{-}\exp(-)dV = -[V\text{-} + (n-1)V\text{-}' + \ldots\ldots$$

$$-(n-1)(n-3)\ldots(2)]PF(V) \quad n \text{ odd and } \geq 3$$

$$= -PF(V) \quad n = 1 \quad (4\text{-}10)$$

and

$$-\int_{1} V\text{-}\exp(\sim)d\frac{V^2}{2} = -[F\text{»} + (n-1)\text{'}\text{-} + \ldots\ldots$$

$$-(n-1)(n-3)\ldots(1)V]PF(V)$$

$$-\backslash\text{-}(n-1)(n-3)\ldots(1)PI(V) \quad n \text{ even and } \geq 2$$

$$= PI(V) \quad n = 0 . \quad (4\text{-}11)$$

For a more detailed mathematical derivation of linearization coefficients Li and Z/2, the reader is referred to reference [21].

4-5 Platform Response Analysis for Surge Motion

Wave forces, including the drag and inertia forces, are computed according to the modified Morison equation. Applicability of Morison's equation is limited to structures in which the diameters of individual members *(D)* are small *(D/L* < 0.2) compared with wave length *(L).* In the case of *D/L* > 0.2, the diffraction effects of members become important.

Figure 4-3 shows the detailed TLP model with four hull and eight column members for the calculation of the horizontal wave forces. The water

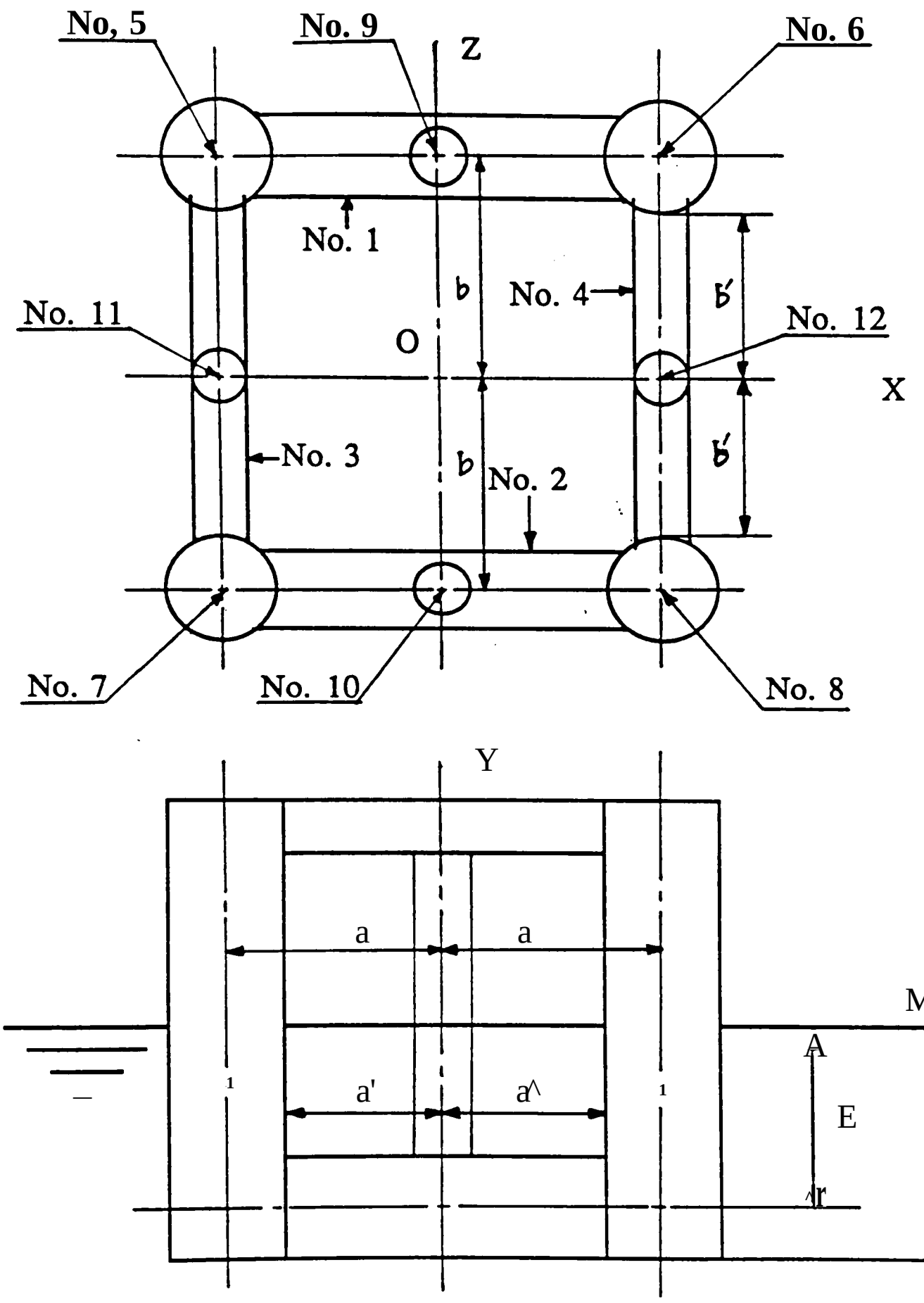

Figure 4-3 TLP model for parameter study

particle velocity and acceleration calculated at the center line of the column and hull members are commonly based on linear wave theory. The horizontal wave particle velocity, *Uw,* and acceleration, $\dot{U}w$, at depth, y, can be expressed as the following equations from the deep water approximations

$$Uw = u\}\frac{IT}{2} e\text{-}\wedge\wedge \cos(Kx - ut) \qquad (4 - 12)$$

$$\dot{U}w = a;2f\wedge e\text{--}\langle\wedge\langle\sin(A'x\text{-}u;0 \qquad (4\text{-}13)$$

where

u; =27r/r : wave frequency

T = wave period

H — wave height

K w u^ Ig : wave number.

The coordinate system (z, *y)* has its origin, O, on the mean water level (MWL) with the positive *y* coordinate directed vertically downward.

4-5-1 Inertia Forces on the Members

The inertia force on the t' th columm is given as

$$Fl = '\wedge pC\wedge D\wedge, j \overset{\cdot hi}{'} \dot{U}wdy \qquad (4\text{-}14)$$

where

p= density of the sea water

CM = inertia coefficient

Di = diameter of the *i* th column.

Substituting Equation (4-13) into Equation (4-14) and integrating yields

$$Fl = \cdot'^{\wedge}PCM9I>^{\wedge}H(1 - c-^{\wedge}'^{\wedge}')sm(\dot{X}x,. - ut) \qquad (4 - 15)$$

where

hi = length of the column under the mean water level.

The total inertia forces on all columns are obtained by summation as

$$Fl, = ^{\wedge}pC^{\wedge}gH'^{\wedge}DUl - e-'"^{\wedge}')sm(K\dot{x}, - ot). \qquad (4 - 16)$$

The total inertia force on the hulls. No. 3 and No. 4, perpendicular to the *x* direction can be written

$$Ffj = \frac{\pi}{2}pCMHD\%e-''''u''b'cos(Ka)s'm(u;t) \qquad (4-17)$$

where

DH = diameter of the hulls

E = depth of the center line of the hulls below MWL.

4-5-2 Drag Forces on the Members

CASE I : Random Wave Only

The drag force on the t' th column can be written as

$$Ff = ^{\wedge}pCoDi \int_{Jo}^{h} I\ Ur.t\ I\ Urei\ \backslash\ dy \qquad (4 - 18)$$

where

CD = drag coefficient

Urei = *Uw* — $\dot{X}$: **random relative velocity.**

The random relative velocity is due to the wave particle velocity and structure velocity. The absolute value of the relative velocity is needed to preserve the sign variation of the force.

The relative velocity square term in Equation (4-18) must be linearized, and the total drag force on all columns for random waves only is calculated by summation as

$$Fl'' = \wedge pCo\ Di\ j\ '\ Ll\ U\wedge\wedge i\ dy \qquad (4\text{-}19)$$

where

L i= *y/2jTi2G^r*

G^r— **standard deviation of relative velocity.**

The standard deviation of relative velocity, a^„ is unknown. This value can be calculated from the root-mean-square value of the relative fluid velocity, as

$$C7_{„} = Uw\ -\ i\ - \qquad (4\text{-}20)$$

The transfer function for the response of the tension leg platform [30] is

$$x = r7G,(u;)c\dot{»}\text{-}* \qquad (4\text{-}21)$$

where

fy= wave amplitude

Q^ **(a;)= appropriate complex frequency response function .**

$$\dot{x} = r/iu;G4u;)e''\text{-}* \qquad (4\text{-}22)$$

Equations (4-20) and (4-22) yield

$$U_r = \bar{U}_w - iuG(uj)e^{i\omega t} \qquad (4-23)$$

where

$$U_r = \frac{U_w}{\eta}$$

$$\bar{U}_w = \frac{U_w}{\eta} .$$

The resultant mean square value of relative fluid velocity is

$$\sigma_r^2 = \int_{Jo} |U_r(w)|^2 S_{\eta\eta}(\omega)\, du, \qquad (4-24)$$

where

$S_{\eta\eta}(u)$ = power spectral density of wave amplitude.

The mean square value of the horizontal wave velocity is calculated from the linear wave theory, and is given as

$$\bar{U}_w = u\omega e^{-Ky} \cos(Kx - \omega t) \qquad (4-25)$$

Therefore, the mean square value of the horizontal wave velocity which changes along the depth y is

$$\sigma_{\bar{U}}^2 = \int_{Jo}^{\infty} u^2 e^{-2Ky} S_{\eta\eta}(\omega)\, d\omega \qquad (4-26)$$

This value is applied to the initial condition because initially there is no relative velocity.

The total drag force on the hulls, No. 3 and No. 4, can be written in the form

$$F\bar{H} = \backslash p \wedge D\ DH\ \mathrm{LI} \int_{J\text{-}b}^{'b'} U\wedge,,dz \qquad (4\text{-}27)$$

where

$L_1 = \sqrt{\frac{2}{\pi}} 2\sigma_{E,r}$

GEr= standard deviation of relative fluid velocity at depth *E* below the mean water level

6' = effective length of hulls in the *z* direction.

The squared standard deviation of the horizontal wave velocity at depth *E* is

$$cl = \int_{Jo} r\ u,''e\text{-}'"'\wedge S,dw \qquad (4\text{-}28)$$

where

E= depth of the center line of the hull below MWL •

This value is applied to the initial condition without relative velocity. The squared standard deviation of the relative velocity, $G\wedge_{\cdot}\ \wedge$, can be calculated by using *E* instead of *y* in Equation (4-26).

CASE II : Random Wave with Current

The drag force on the t' th column for random waves with current is expressed as

$$Ff = \backslash pCo\ Dij'l \int_{\cdot}^{h} Ur.1\ \mathrm{I}\ C/_{„}\ \backslash dy \qquad (4\text{-}29)$$

where

$Ur\wedge, = Uc\text{-}tr(t)$

$r\{t) = Uw - i$

Uret= total relative velocity

r(t)= random relative velocity between the wave particles and the structure

Uc = current velocity.

The relative velocity squared term in Equation (4-29) must be linearized. The drag force on the columns is then obtained as

$$Ff = \backslash pCo\ Di\ [U, I \int^{'hi} L:,dy -\backslash- 1 \int^{fhi} L, U\wedge.\wedge dy], \qquad (4-30)$$

The total drag force on the hulls in the case of random wave with current velocity can be expressed by

$$FS = pCo\ DH\ [La\ 17c + Ll \int_{J-b'}^{rb'} L\wedge_{,,} dz]. \qquad (4-31)$$

4-5-3 Total Forces on the Members

The total force F, on the column and hull elements for surge motion can be found simply by summing the drag and the inertia forces, as given by the following general equation:

$$F, = H[F,i\ cosut - F,2\ smiut] -\backslash- F\wedge n \qquad (4-32)$$

where

$$F_{.,} = J/>C«<?X;\wedge(l-«'''''')\sin(/fxO \quad \sum_{i=5}^{12}$$

$$F_{,,} = \frac{\pi}{8} -pCugf\wedge Dni-'-''''')cos\{Kx,) \sum_{i=5} + \wedge pCDle-'''\wedge H'cos\{Ka)$$

and $F\wedge D$ is the total drag force as given by

CASE I : Random Wave Only

$$F.D = \text{-ZPCD } \sum_{i=s}^{J} y^{\wedge} Di \; / \; L^{\wedge} Ureidy - ^{\wedge} pCDDnLi \; / \; Ureidz$$

CASE II : Random Wave with Current

$$F.D = :ZPCD \; \frac{1}{2} \sum_{\wedge}^{\wedge} A \; [UC \; I_{Jo}^{f^{\wedge *}} L^{\wedge} dy - ^{\wedge} r \; / \; \int_{Jo}^{r^{\wedge *}} L,U,,idy] + pCnDh \; [L^{\wedge} U^{\wedge} + L, \; / \; \int_{J-b'}^{f^{\wedge '}} U^{\wedge\wedge\wedge} d^{\wedge}.$$

The force terms related to the current velocity are applied to calculate the response of current velocity. The random wave force terms are applied to spectral analysis mentioned in the following section. Equation (4-32) can also be written as

$$F, = HFA \cos(ut + <^{\wedge},) + F^{\wedge} D \qquad (4 - 33)$$

where

$$FA = \sqrt{F^{\wedge}, + Fl,}$$

$$\tan(f>^{\wedge} = \frac{F}{F_{x1}}.$$

4-5-4 Transfer Function for Wave Height

The spectral density of the wave loading *SFX* (w) can be related to the wave spectral density through the transfer function *Gp (u)*. The transfer function that relates the height *H of a* wave to the loading it causes on a structural member is *Gp (u)*. Transfer functions of the harmonic form are defined as

$$GF(U) = GjroC^{*''*} \qquad for- \quad i = V^{\wedge} \qquad (4 - 34)$$

where

GFO= complex number independent of time .

Since a simple wave is harmonic, the forcing function F, (t), which consists of fluid inertia and drag forces, can be written in the form of Equation (4-33). The connection between a forcing function and its transfer function is defined [36] as

$$\textit{(Forcing function)} = H \times \textit{real}\,[GF\,(w)]. \qquad (4 — 35)$$

Equations (4-33) and (4-35) yield

$$GF\,(w) = F^{\wedge}\cos(ujt + <?^{\wedge *}) + {}^{\wedge}. \qquad (4\text{-}36)$$

From Equation (4-35) the structural forcing function can be redefined in terms of the transfer function [36] as

$$F. = ri(t)\backslash Gr(u)\backslash. \qquad (4\text{-}37)$$

The wave amplitude, *T)(t),* which is a stationary random process with a zero mean and with a spectral density, 5'„(u;), is assumed to be a distribution of linear waves.

From the basic definitions of the autocorrelation function and the spectral density function, the spectral density of the wave force, *SFx(^)i* is related to *Sr, (u)* through the known transfer function *GF* (w) [36]

$$SFX(\hat{})=|GF(U)|' \; S,(u;), \qquad (4\text{-}38)$$

4-5-5 Spectral Analysis for Surge Response

The equation of motion of a single^degree-of-freedom (SDOF) system for a structure is derived by considering the equilibrium of forces on the tension leg platform. The structure is subjected to a restoring force due to the horizontal component of the tether tension and an external force induced by waves and the current. But the hydrodynamic damping for a viscous force representing structural damping can be neglected in surge motion, since the surge periods of oscillation are of the order of 60 s, and thus resonance due to ocean wave excitation is extremely unlikely. Therefore, the equation of motion in the horizontal, or *x* direction is

$$m,\ddot{x} + A_{x}x = F\hat{}(t) \qquad (4\text{-}39)$$

where

m . = *Mp -{-Max*

M_{p} = structural mass of the tension leg platform

M_{ax} = added mass due to columns and hulls in the x direction.

The added mass for the columns and hulls can be calculated by the following equation.

$$M_{\text{„}} = \pi J/.[C.c \sum_{\text{»}=6}^{12} X; r>fK + 4C,H\,DI\,b'] \qquad (4-40)$$

where

Gac = added mass coefficient for columns

CaH = added mass coefficient for hull at depth E below the mean water level. The added mass coefficient for the rectangular hull was experimentally determined by Chung [49].

In order to carry out a frequency domain solution of the surge response, the relationship between response spectral density, ^^.(a;), and the variance, a^, from Equation (4-39) is required. The harmonic response function *H(uj),* sometimes called the frequency response function, for the equation of motion is calculated by

$$^M = \frac{1}{m,(wj - u;2)} \qquad (4-41)$$

where

w« = $\overline{y/k/m^{\wedge}}$: circular frequency of the structure .

The response spectral density, 5,(0;), can be calculated from the frequency response function, *H(u)f* which is the Fourier transform of the impulse response function, *h(t)*^ and the spectral density of the wave loading, 5jr,(a;), by using the definition of spectral density and autocorrelation

$$S,(u)=\backslash H(u)\backslash^{\wedge}\ Sp^{\wedge}(u;), \qquad (4-42)$$

Substitution Equation (4-38) into Equation (4-42) gives

$$5.(w) = 1\ ff(u.)\ n\ GF(U.)\ I'\ S,(u). \qquad (4 - 43)$$

Theoretically, the mean square value of TLP response requires integration of the corresponding response spectrum 5, *(u)* over the whole frequency range, —oo < a; < oo

$$GI = \int_{J-oo}^{} S^{(uj)du}, \qquad (4-44)$$

However, for numerical integration purposes, a finite frequency range with cut-off points can be used. Most response spectra become extremely small at moderate frequencies, and beyond those frequencies the energy spectrum is negligible.

Briefly, the procedure of frequency-domain analysis for TLP response is summarized as the following steps.

1) **Decompose the input wave height spectrum into the proper number of frequency.**
2) **Calculate the drag and inertia forces on the structure members.**
3) **Calculate the transfer function and the spectral density for the wave force.**
4) **By using the definition of the spectral density and the autocorrelation, find the spectral density of the structure response.**
5) **By integrating the corresponding response spectrum over the whole frequency ranges and calculating the root of the integration value, find the standard deviation value of TLP response. Now the first iteration is**

completed. For the next iteration, the structure will have a velocity. Hence, the relative velocity should be included in the calculation.

6) Return to the step 2) until the standard deviation response of structure is converged.

CHAPTER V

NUMERICAL EVALUATION

5-1 Introduction

Parameter values for the numerical studies of a TLP surge response are determined and evaluated in this chapter. The basic data of structural configuration are the same as those of reference [50]. The environment for the TLP design is employed in the condition of an extreme sea state in the North Sea. Becaifee the expected maximum dynamic response of a TLP due to an extreme sea state is required for the design in the location of the TLP, the numerical developments of the frequency domain analysis in both random wave only and random wave with current are focussed on the dynamic surge response of the TLP. The effect of the relative velocity on the hydrodynamic force equation is considered. The results of the responses due to the presence of current velocities are also calculated and discussed.

5-2 Parameter Data

5-2-1 Platform and Tether Data

The TLP model for the numerical studies is shown in Figure 4-3. The corresponding data of structural configuration are listed in Table 5-1. The data for the tensioned steel tethers at the four corner columns are also listed in Table 5-1.

Table 5-1 Parameter values for platform and tether

Total structure mass	31200 tons
Diameter of corner columns	16 m
Spacing of corner columns	70 m
Length of hulls	54 m
Diameter of hulls (No. 1, 2)	14 m
Diameter of hulls (No. 3, 4)	6 m
Diameter of cross braces	3.5 m
Submerged depth	35 m
Tether length	125 m
Tether stiffness per leg for surge	205000 N/m
Tether tension per leg	2560 tons (force)

5-2-2 Environmental Data

The North Sea is chosen for the environmental location where the water depth is 160 m. The modified JONSWAP wave spectrum, which is expressed in terms of the significant wave height and the significant wave period, is used for random sea states in the frequency domain analysis.

The current velocity profile is considered to be steady in time and uniformly distributed in depth. The input data of the current velocity profile has the following cases:

case 1 = 1 knot (0.515 m/s)

case 2 = 2 knot (1.03 m/s)

case 3 = 3 knot (1.545 m/s).

The data for the significant wave height and the significant wave period are the following:

wave height = 30 m

wave period = 17 s.

5-3 Numerical Results

The cut-off frequencies used for numerical calculation are

cji = 0.2 rad/s

***ijj2* = 1.2 rad/s**

where

*(jj^* =low limit

u-i =high limit.

This frequency range is decomposed into 101 component frequencies for the linearized frequency domain analysis. Number of frequencies, 101, is chosen from reference [50] which dealt with frequency-domain analysis for offshore structure response. The procedure for frequency domain riser analysis for a random wave with no current is explained by Krolikowski and Gay [19]. This procedure also can be applied to the TLP model for frequency domain analysis.

In the case of random waves with a steady current, the wave characteristics due to wave-current interaction are changed. The wave energy loss due to the decrease of wave height reduces the standard deviation response of structure because the current is the same direction as the waves, which is the worst case in sea. The fiow chart for frequency domain analysis is shown in Figure 5-1.

The numerical calculation is performed on the IBM-3081 computer, and the results are plotted on the same computer. Figures 5-2, 5-3, and 5-4 show the change of input spectrum due to different current velocities in Equation (3-8). Figures 5-5, 5-6, 5-7, and 5-8 show the transfer function for fluid inertia and drag forces, which is defined in Equation (4-36), in the case of random wave only and random waves with three different current velocities. The transfer functions for the surge response of the TLP, which is related to Equation (4-43), in the C2ise of random waves only and random waves with current are shown in Figures 5-9, 5-10, 5-11, and 5-12. Although the transfer functions for fluid force and structure response all look similar despite

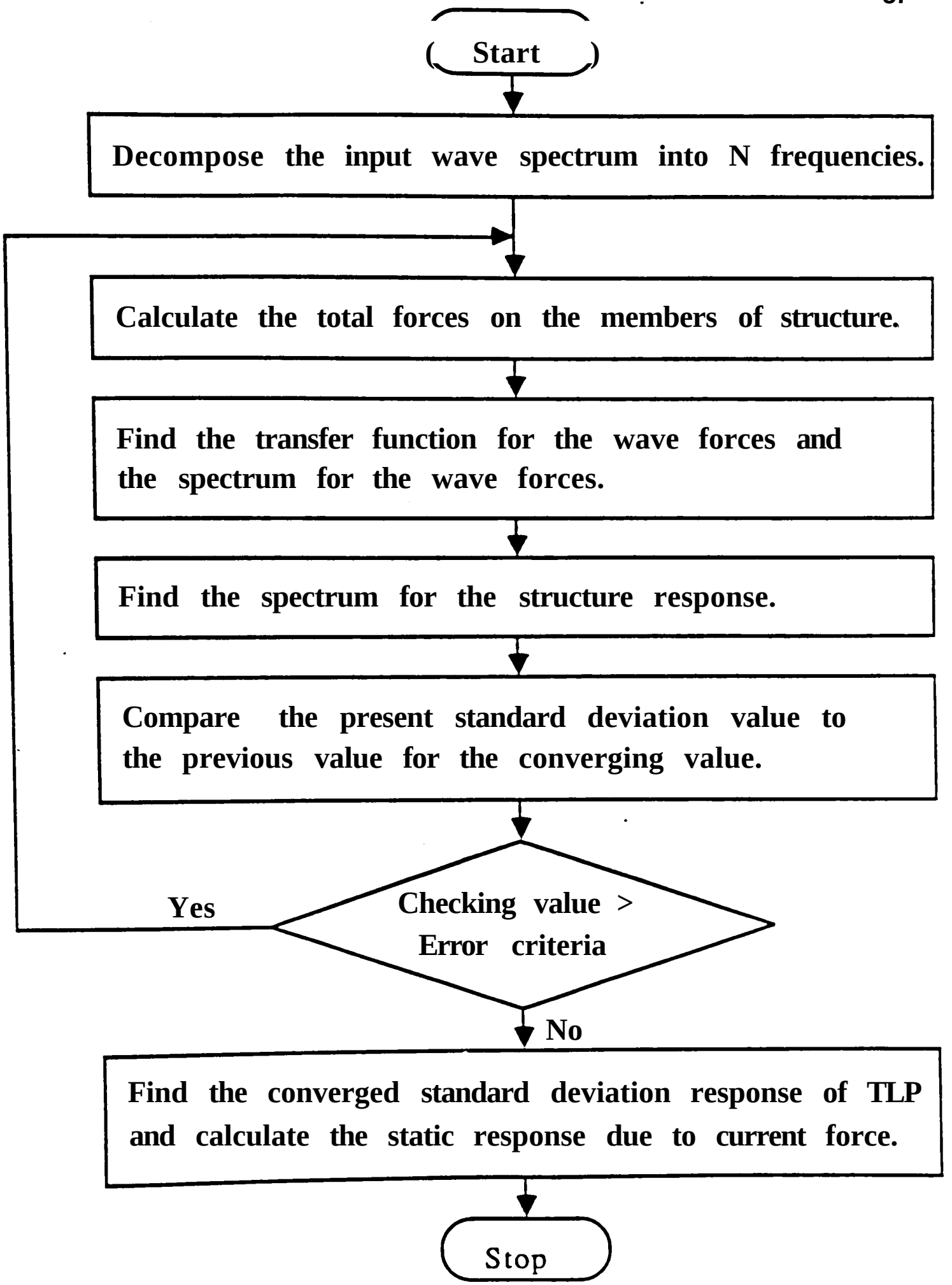

Figure 5-1 Flow chart for frequency-domain analysis

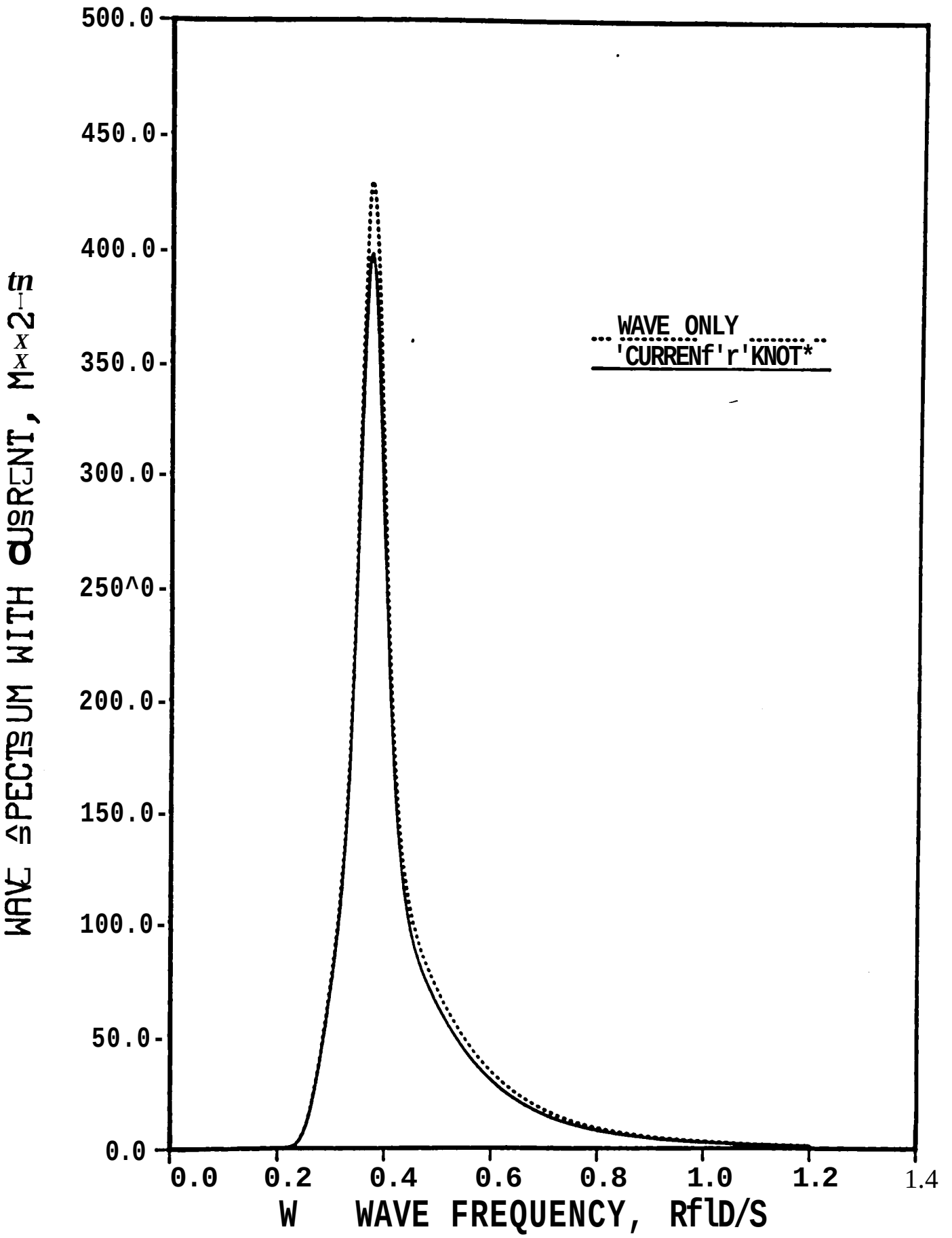

Figure 5-2 Random wave-current interaction spectrum with current velocity, 1 knot

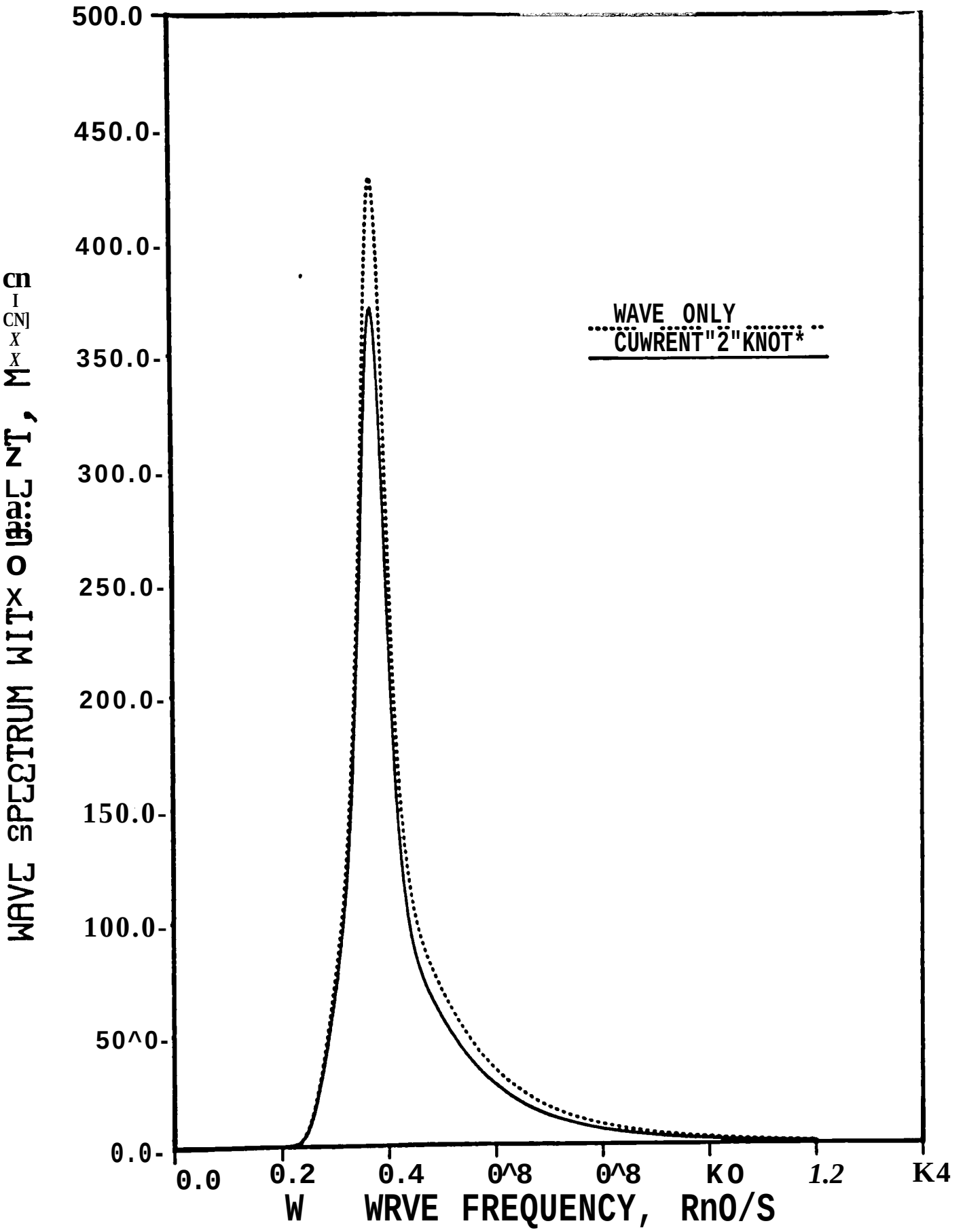

Figure 5-3 Random wave-current interaction spectrum with current velocity, 2 knot

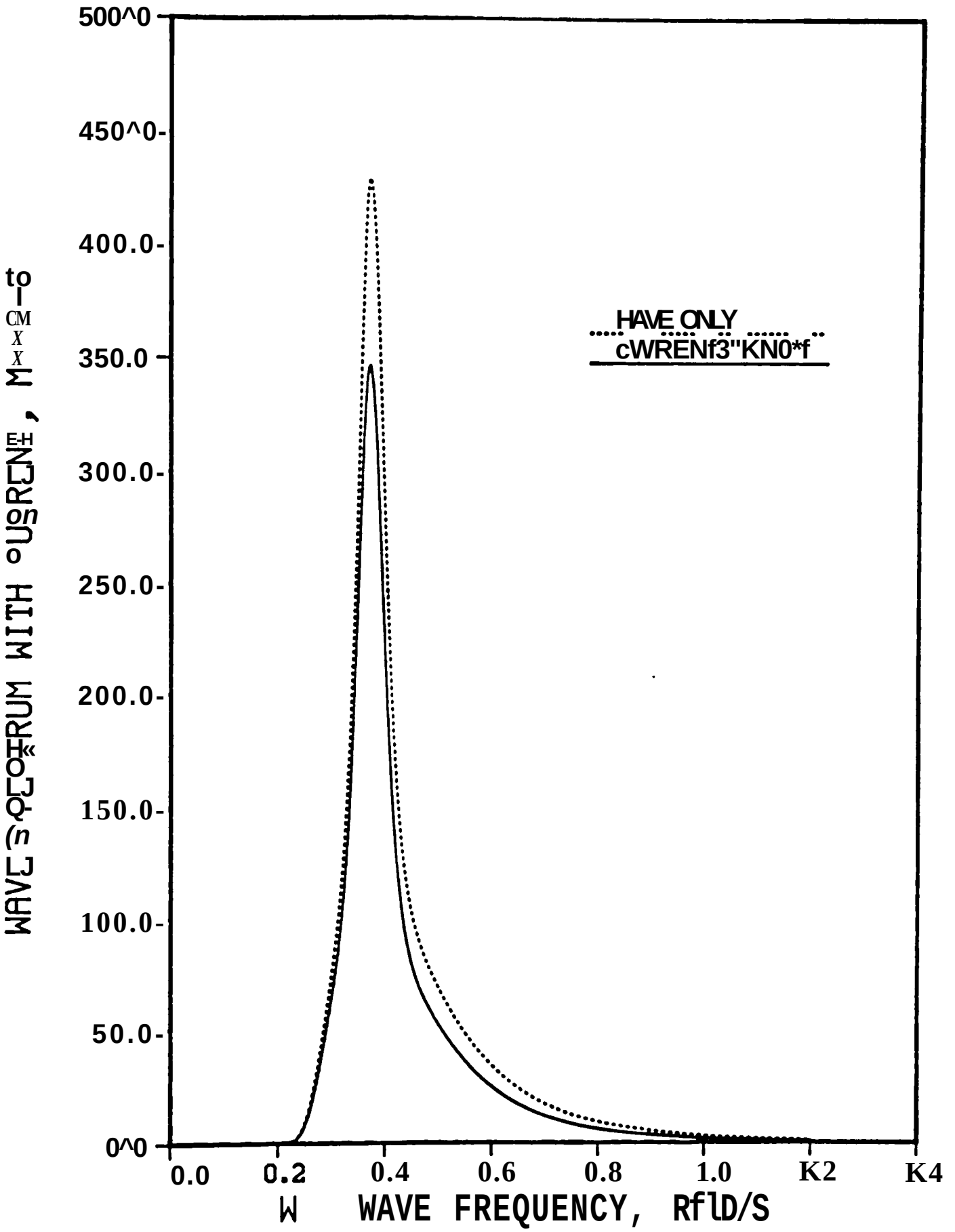

Figure 5-4 Random wave-current interaction spectrum with current velocity, 3 knot

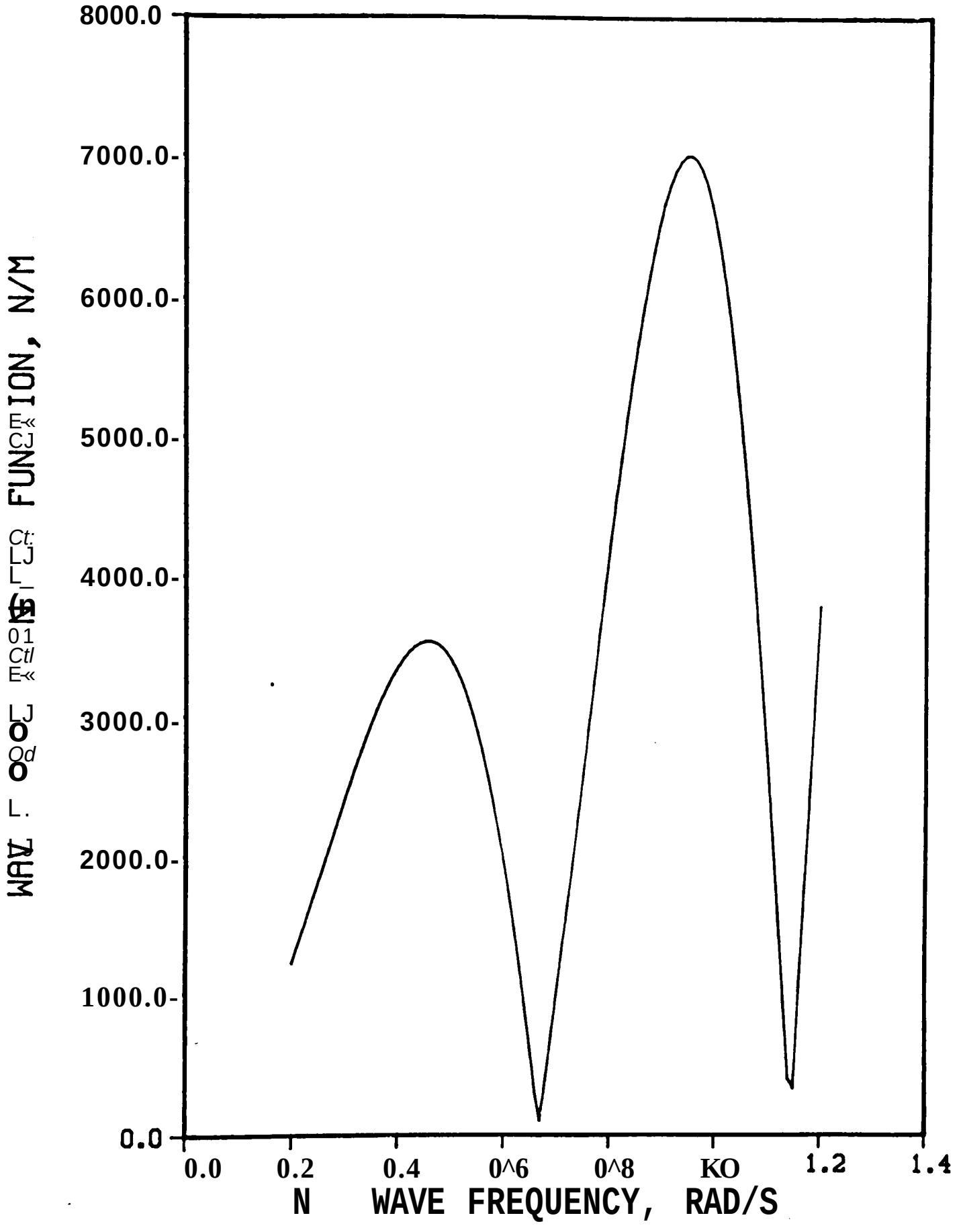

Figure 5-5 Transfer function for random wave force

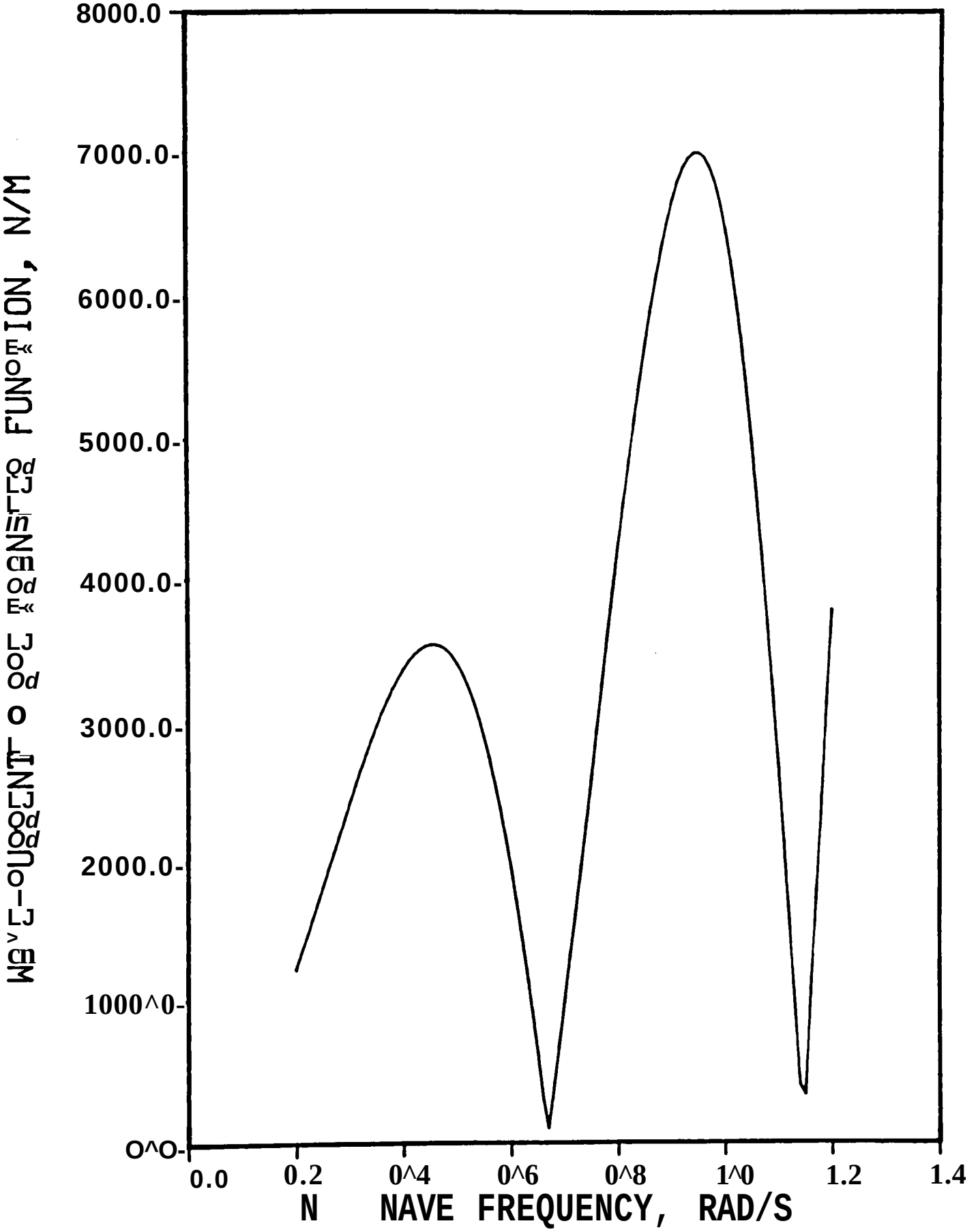

Figure 5-6 Transfer function for random wave-current interaction force with current velocity, 1 knot

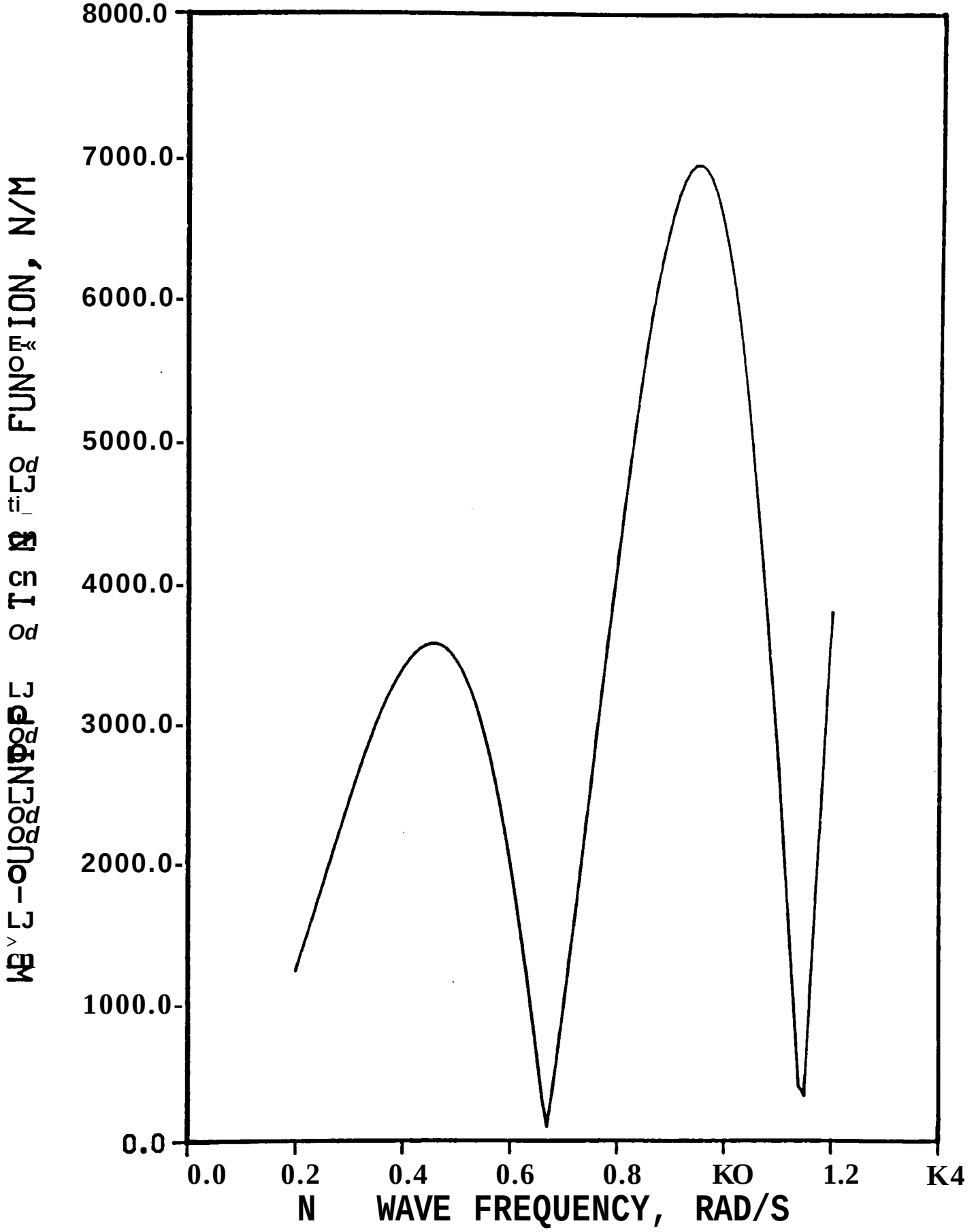

Figure 5-7 Transfer function for random wave-current interaction force with current velocity, 2 knot

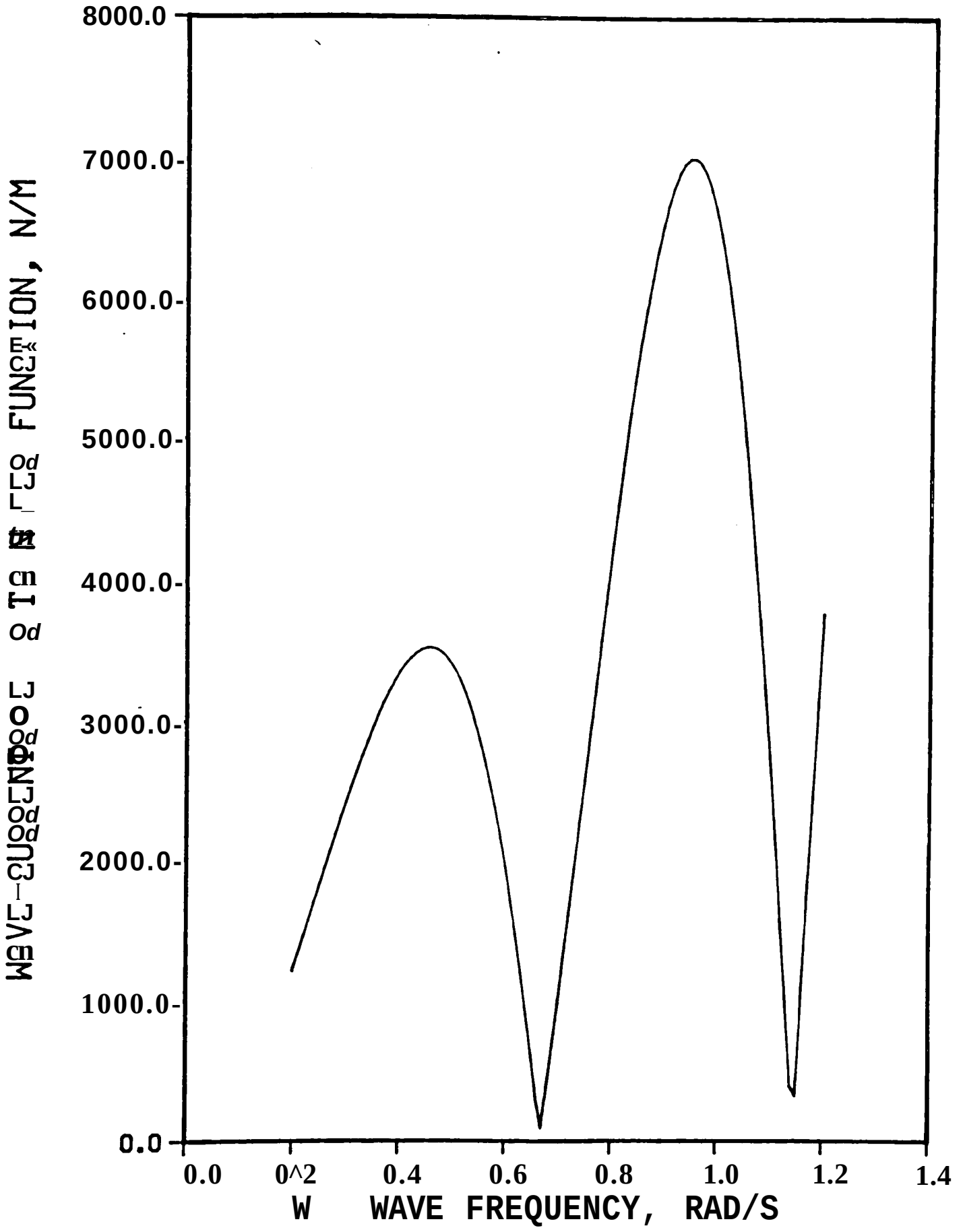

Figure 5-8 Transfer function for random wave-current interaction force with current velocity, 3 knot

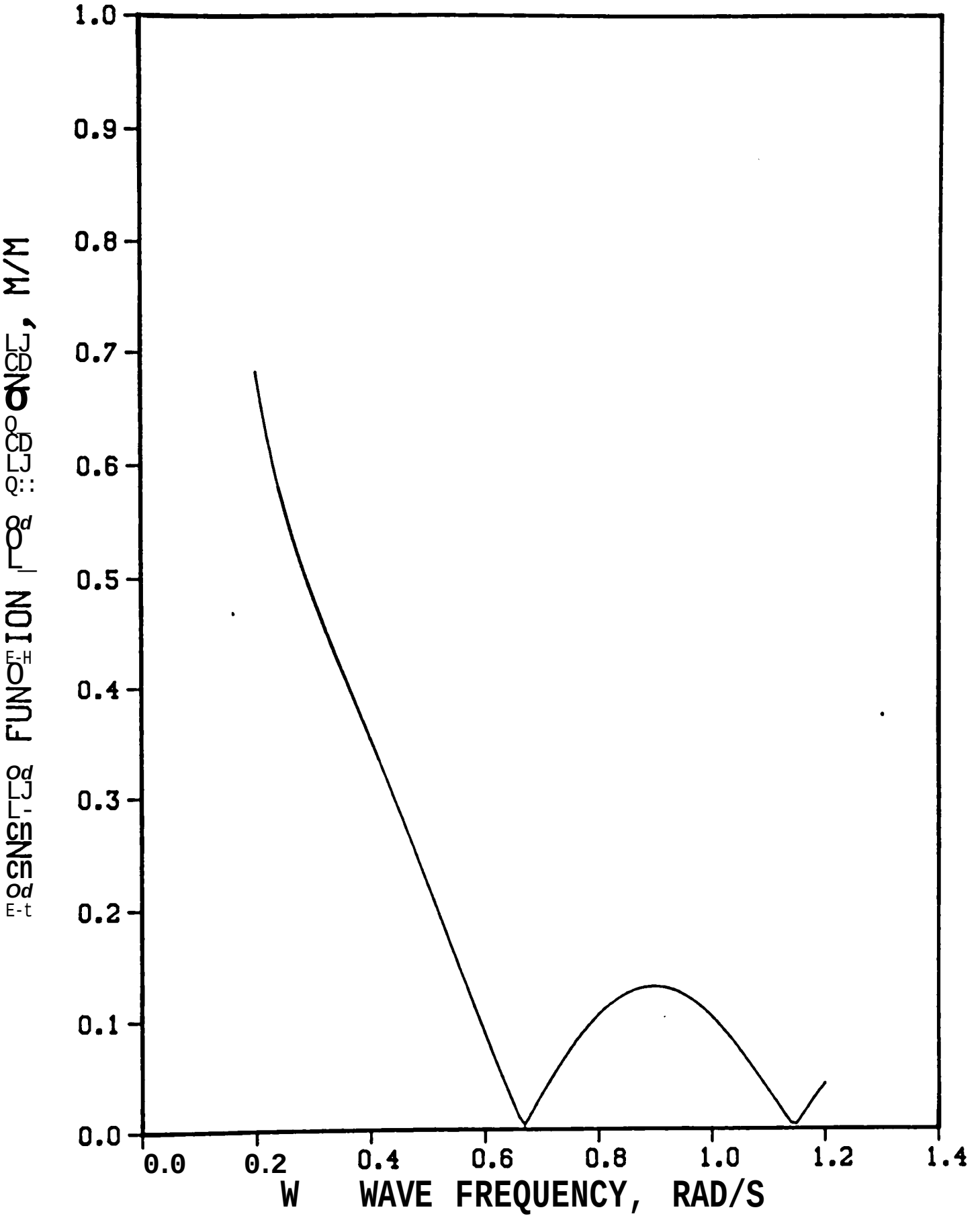

Figure 5-9 Transfer function for TLP response in random wave only

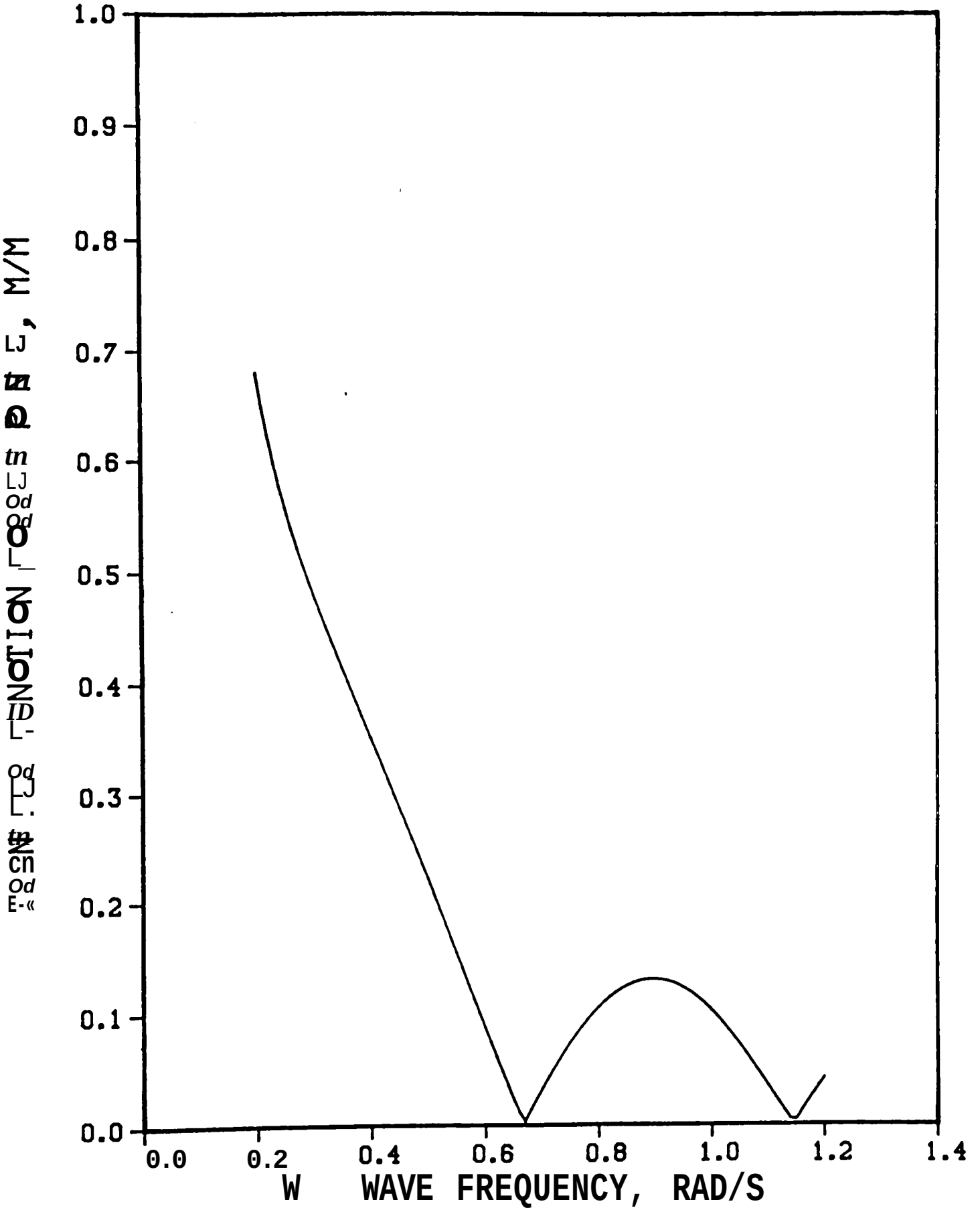

Figure 5-10 Transfer function for TLP response in random wave with current velocity, 1 knot

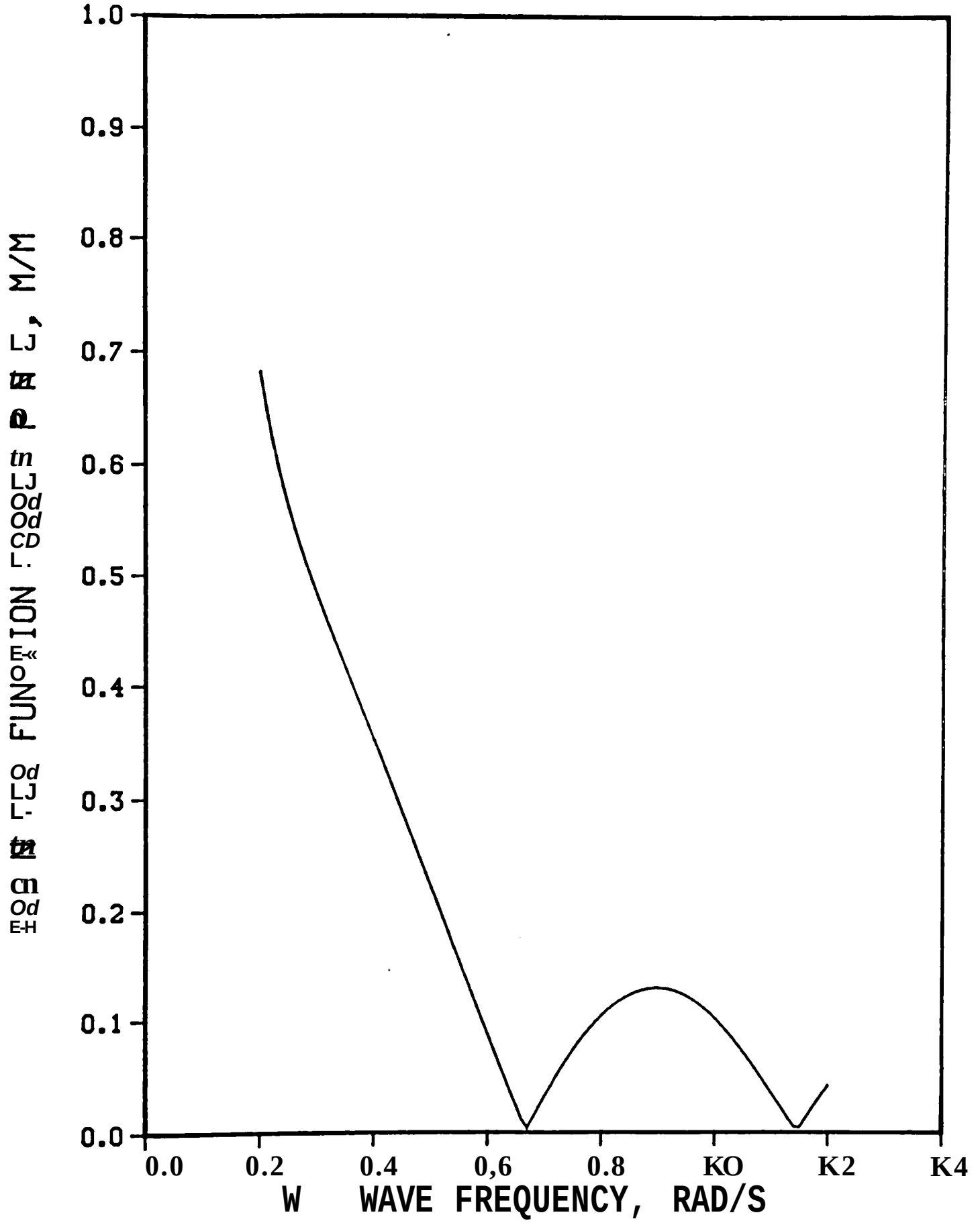

Figure 5-11 Transfer function for TLP response in random wave with current velocity, 2 knot

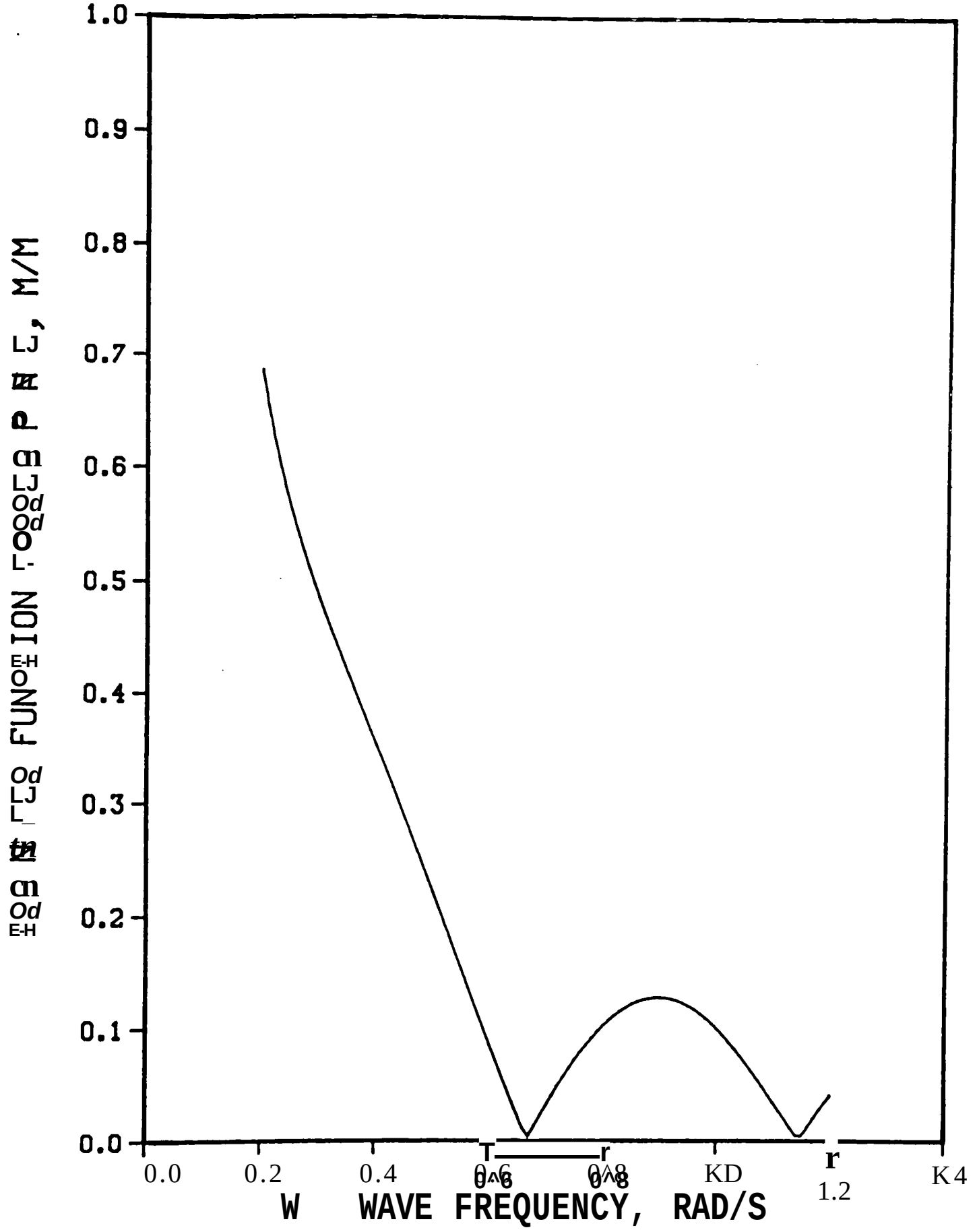

Figure 5-12 Transfer function for TLP response in random wave with current velocity, 3 knot

different input spectra due to different current velocities, the response spectra, 5, (cj), for structure response analysis are different as shown in Figures 5-13, 5-14, 5-15. The effect of static current velocity on the structure response will be mentioned in the following section.

5-4 Discussion

The current velocity is related to the hydrodynamic drag force, which creates the nonlinearity of offshore structure dynamic analysis. Therefore, a linearized version of the nonlinear drag term in Equation (4-4) has two different terms. The first term contains the constant input of current, and the second term has the random process due to random sea or random modification of wave-current interaction. The analysis for the random process can be explained by the spectral analysis of random vibration. The effect of constant input can be explained by static analysis.

Table 5-2 shows the standard deviation response of the surge motion in the case of wave only and random wave with current. The standard deviation response is decreased due to the wave-current interaction, and the mean response is the effect of static current velocity. The mean response of TLP is calculated at the origin of x—y coordinate shown in Figure 4-2, and the the dynamic response is superimposed on it.

In the wave only case, the standard deviation amplitude of the surge motion is 2.628 m without the consideration of relative velocity and 2.717

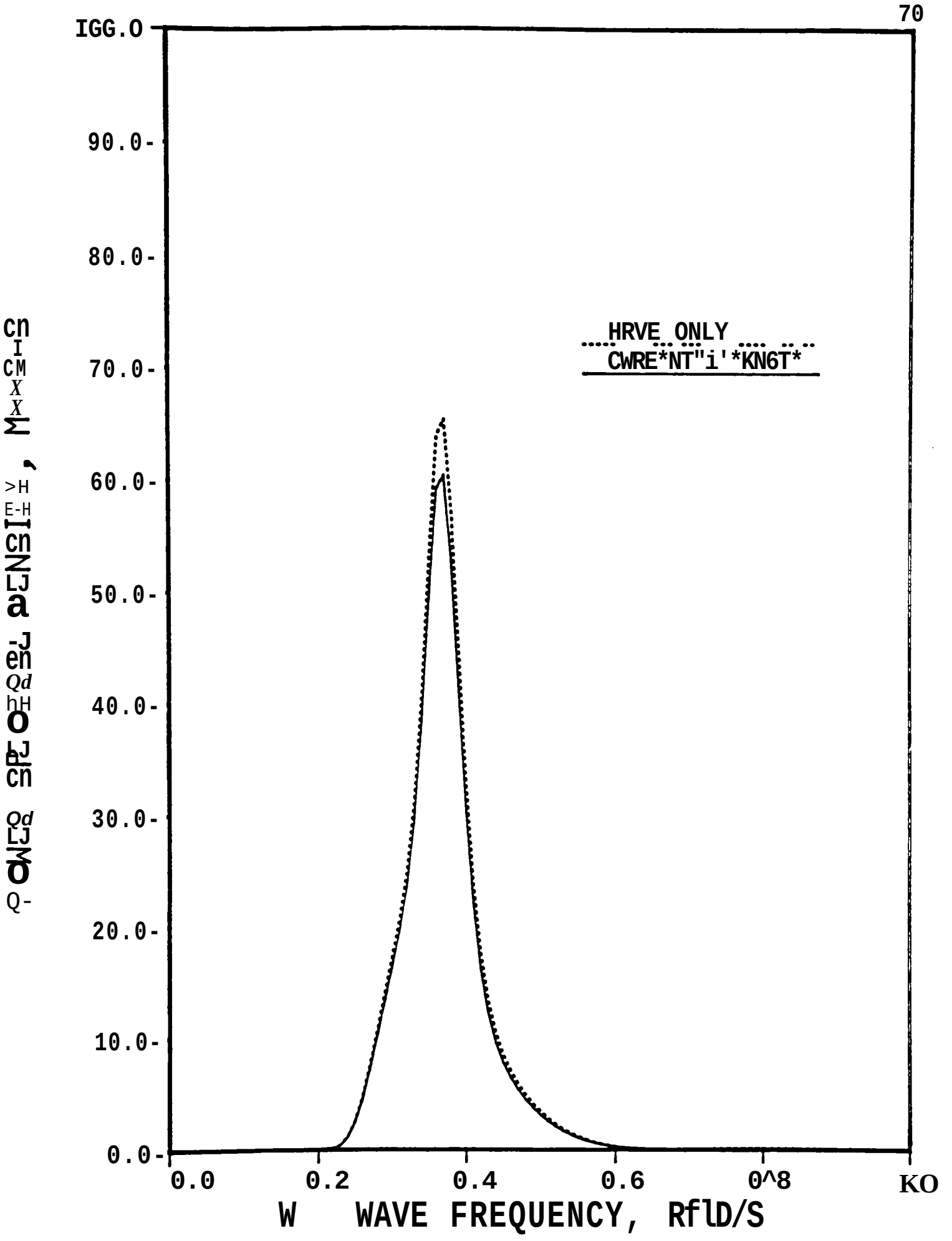

Figure 5-13 TLP response spectra for random wave and random wave with current velocity, 1 knot

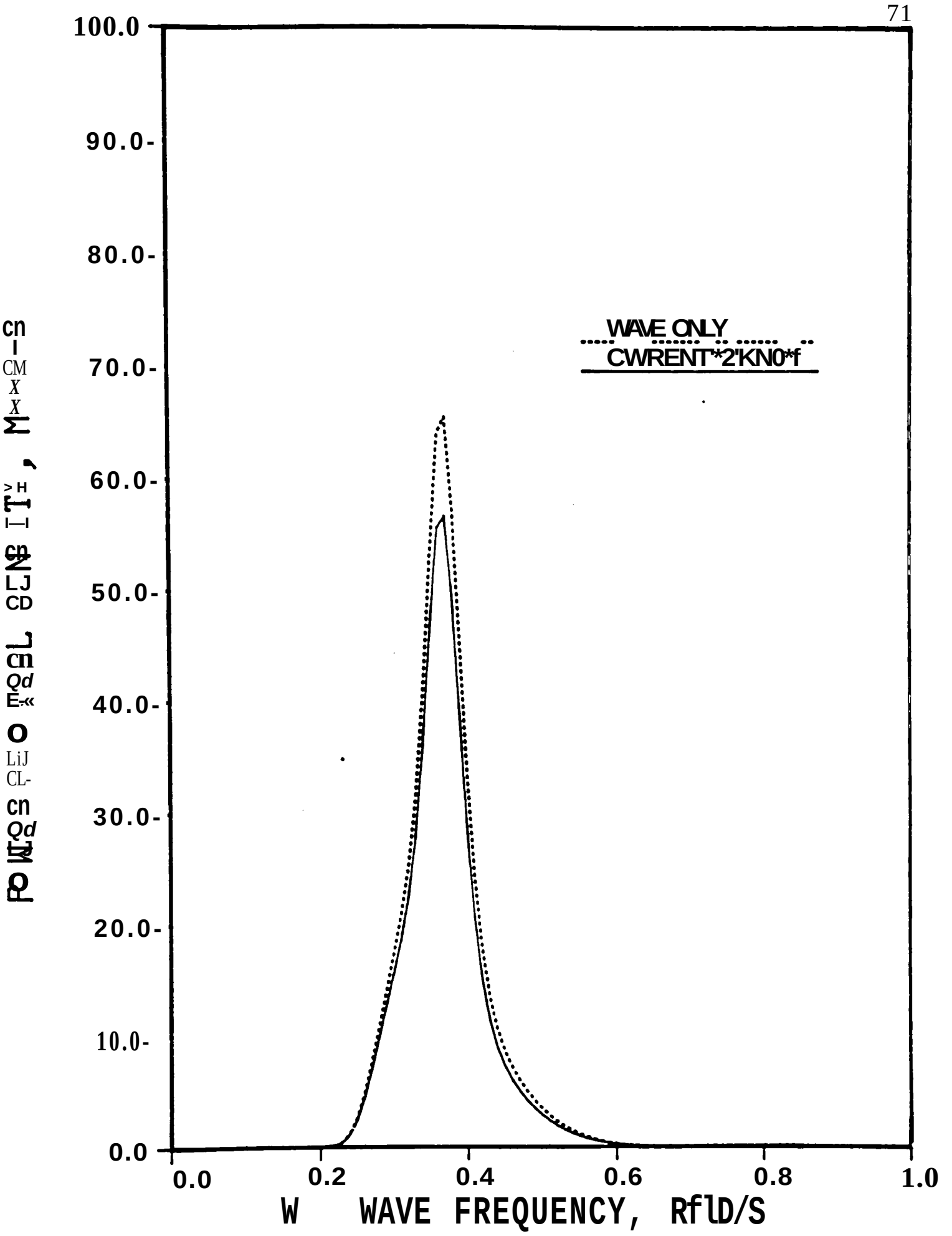

Figure 5-14 TLP response spectra for random wave and random wave with current velocity, 2 knot

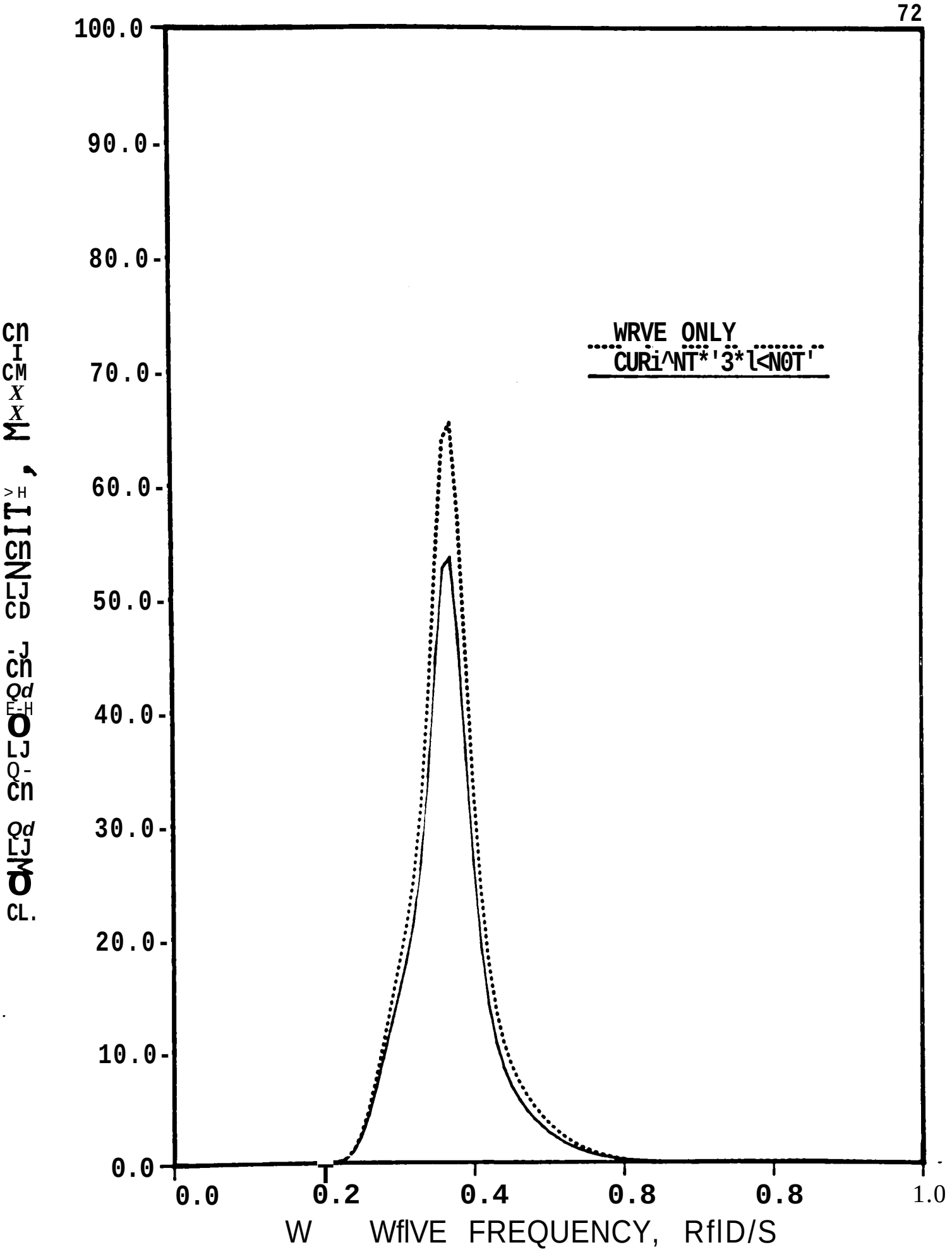

Figure 5-15 TLP response spectra for random wave and random wave with current velocity, 3 knot

Table 5-2 Results of surge response in frequency-domain analysis

		Standard deviation response (m)	Mean response (m)	Expected maximum response (m)	CPU time (sec)
Random wave only		2.628	0.0	13.403	1.82
Random wave with current profile	1 knot 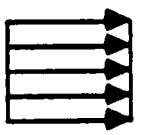	2.527	3.254	16.142	5.71
	2 knot 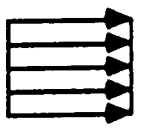	2.439	6.301	18.740	5.71
	3 knot 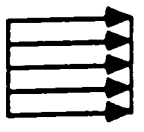	2.361	9.296	21.337	5.71

m with the consideration of relative velocity. These data represent the difference as a result of including relative velocity due to TLP and wave particle velocity.

Ochi [51] developed the formulas for predicting the extreme value of the maxima of a stationary random process that would occur in a certain period of time during which the sea environment was constant. He applied the estimation formulas to predict the extreme value of the pitching motion and acceleration of a ship in irregular sea waves generated in a towing tank and found that the extreme values observed in model tests were very similar to the predicted most probable values. The maximum predicted surge displacement of the TLP is based on Ochi's formulas. For a storm of 12 hours' duration, using a peak wave spectrum period of 17 s, a wave height of 30 m, and the probability that extreme values exceed a specified value as 0.01, the ratio of the extreme value to the root mean square for the stationary Gaussian random process from Ochi's formulas yields a ratio of approximately 5.1 [50], Therefore, the expected maximum response of TLP can be calculated by multiplying the standard deviation response by Ochi's ratio, 5.1, and adding the mean response due to current effect.

5-5 Conclusions

The infiuence of the surge response of relative velocity due to water particle velocity and TLP velocity is significant in the view of the maximum expected response. The presence of current velocity in the frequency domain

analysis has a strong influence on the TLP surge motion. Surge motion, which can cause stretching of the tensioned cables and the underbuoy riser is an important parameter.

CHAPTER VI

RANDOM TIME-DOMAIN SIMULATION

6-1 Introduction

All phenomena in nature have random environmental factors that are difficult to represent by any simple function or any simple combination of functions. Offshore engineering deals with these kinds of random analysis. In this area, stochastic analysis can satisfactorily describe the ocean phenomena, especially sea waves. But the statistical properties of sea waves make the response analysis of offshore structures quite complicated and usually make the analytical solution of the statistical characterization of the response impossible. Also, loads induced by ocean waves have the nonlinearity created from the square term of random relative velocity due to water particle velocity and response velocity.

An alternative approach to determining the exact response statistics of nonlinear, structural systems is simulation technique. Simulation techniques are based on artificial data that can be generated from digital computer. The major goal of this chapter is to determine response statistics of TLP's due to random wave simulations using the superposition method, one of the simulation techniques. The statistical analysis is also explained in the case of random value with constant current velocity.

6-2 Literature Survey

The purpose of this section is to survey the literature concerning time-domain analyses of offshore structures with raindom waves. This survey can help the reader review the primary interests and recent developments in offshore engineering.

Borgman [52] applied digital time sequence simulations of random waves to ocean engineering and investigated possible ways of increasing the efficiency and the realism of the ocean wave and force simulations. Two basic methods, wave superposition and linear filtering, were studied for simulating ocean wave processes.

Burke and Tighe [53] presented an analytical study on evaluating the dynamic response of fixed offshore structures due to earthquakes and storm wave and analyzed the time series of the nonlinear equation of motion by using a digital computer. Wave velocities and accelerations were simulated by using the power spectral density of a Pierson-Moskowitz spectrum for the random sea generator.

Godeau et al. [54, 55] developed a mathematical model that simulated the dynamic behavior of an offshore fixed platform in the time domain and presented its application to an actual North Sea platform. The results from the integration of a nonlinear system were interpreted to the maximum stress level related to an extreme sea state and the fatigue level of the structure.

Hudspeth [56] simulated a nonlinear random time sequence of a surface gravity wave spectrum in a finite ocean depth by using a fast Fourier transform algorithm. This nonlinear random sea time sequence was filtered by the linear digital filter method in order to compute the kinematic fields required in the Morison equation. The results were compared with measured pressure force spectra in the Gulf of Mexico.

Hudspeth and Chen [57] developed a method to extend the digital simulation of unidirectional random sea to second order for some improvement in the prediction of random wave forces. Also, a finite Fourier transform algorithm was adopted to simulate a discrete, unidirectional, nonlinear, random sea surface by a digital computer. Hudspeth and Borgman [58] developed methods for stacking the discretized time series, which required only half the computer core storage compared to the unstacked finite Fourier transform algorithms.

Shinozuka et al. [59] investigated the response of an offshore tower due to short-crested and long-crested ocean waves in a time-domain analysis. Time histories of the water particle velocity and acceleration for ocean waves were numerically generated by different mean wind velocities, and time histories of the tower response due to long-crested and short-crested seas were developed.

Spanos and Hansen [60] presented an alternative method of simulating sea wave records based on the Linear Prediction Theory (LPT). Records of sea waves possessing a power spectrum are obtained as the output of a

recursive digital filter to a white noise input. The applicability of the proposed method was examined in simulating wave velocity and wave acceleration records.

Spanos [61] developed three different classes of numerical schemes, namely autoregressive (AR) algorithms, moving-average (MA) algorithms, and autoregressive moving-average (ARMA) algorithms, for simulating a time series compatible with a given target power spectrum of ocean waves. The Pierson-Moskowitz spectrum was adopted for numerical computations. Applicability to ocean engineering problems was also discussed.

Lin and Hartt [62] presented a time-series simulation method, which was based on the principle of time series modeling for dynamic systems, for a long-term simulation. The time series obtained by summing the Fourier components corresponding to the power spectral model were useful for a short-time simulation. The applicability of the proposed method to long-term, high-cycle fatigue testing was also presented by example.

6-3 Simulations for TLP Surge Response

The sea surface elevation equation in this research is assumed to be a stationary, ergodic stochastic process. There are two basic methods of simulating ocean wave process in time history: wave superposition and linear filters. Although each technique has advantages and disadvantages, both methods seek to produce a mean zero, Gaussian stochastic process, which has

an initially specified function as its spectral density. In this thesis, the wave superposition method is adopted for stochastic time-domain analysis.

From linear wave theory, ocean waves can be simply represented by sinusoidal motion. Although this simplification analytically makes analysis of offshore phenomena easy, the real data of ocean waves represent unpredictable curves. These curves can be similarly obtained by superposing many sinusoidal curves with random phase angles that are uniformly distributed in the range of (0, *2ir).* For generating uniform distribution for random phase angles, the IMSL (International Mathematical and Statistical Library) subroutine GGUBS (basic uniform pseudo-random number generator) may be used to generate a sequence of random numbers which have zero mean and unit standard deviation. The random numbers between (0,1) are extended to the random numbers between (0, *2ir)* by multiplying by 27r. The superposition simulation is based on the superposition of many waves, each having a random phase angle and an amplitude consistent with the input wave energy density spectrum at that frequency. Following is an explanation of the procedures for developing simulations and the methods by which simulated wave particle velocities and accelerations are applied to TLP's for structure surge response.

First of all, the input wave energy spectrum is divided into several parts as shown in Figure 6-1. For numerical convenience, the input spectrum can be divided equally. Each division contains a sufficient number of components,

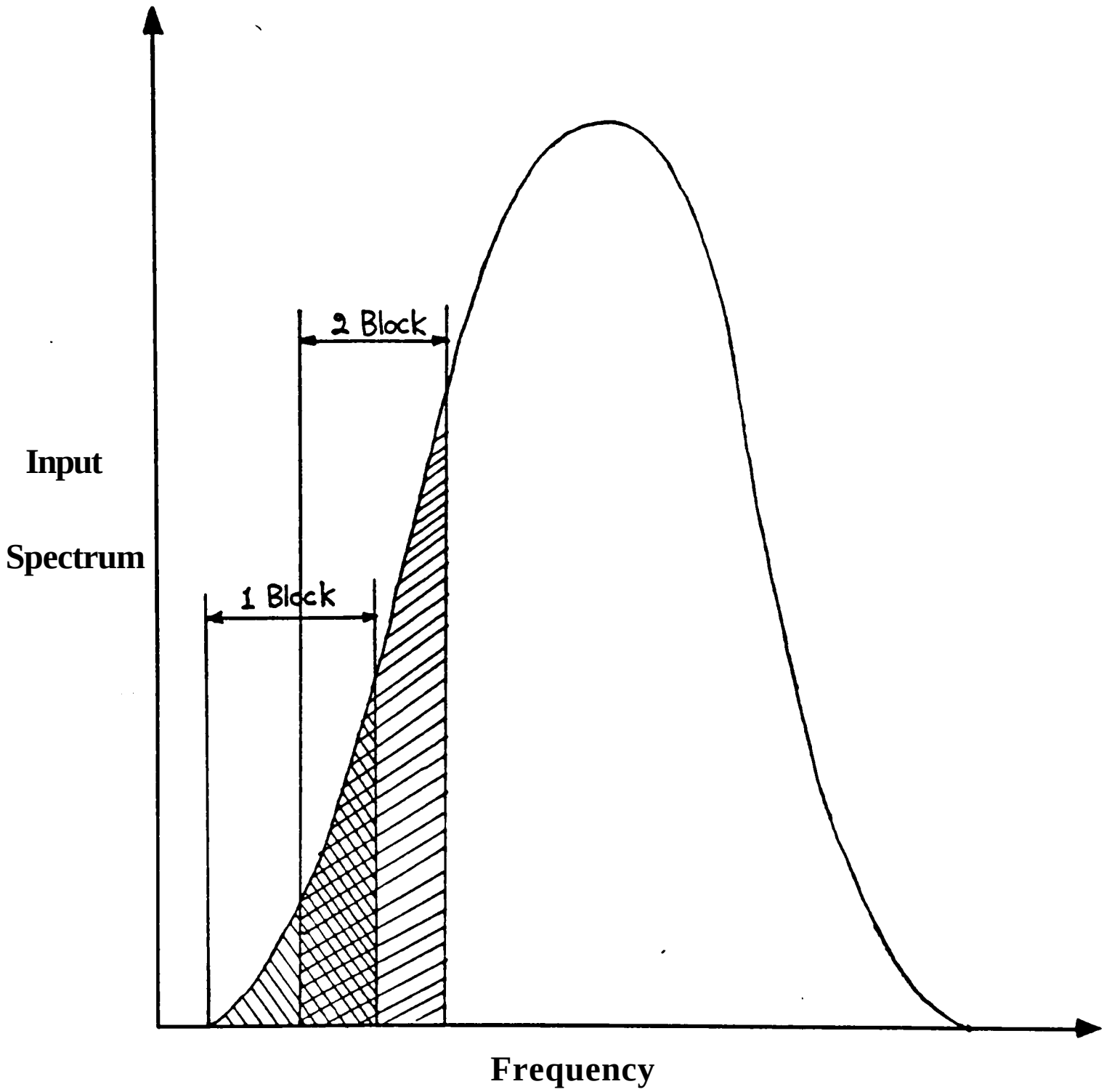

Figure 6-1 Divisions of input spectrum for time simulation

A(j, which is at least 50, to assure randomness. The use of about 200 components duplicates two divisions among several divisions of the input spectrum accurately [63]. The values calculated at every division are averaged over the number of total divisions. This method is widely used in simulating random waves for a given wave energy spectrum. The wave elevation, wave velocity, and wave acceleration simulations will be numerically developed with the input wave energy spectrum.

Numerical calculations are carried out for a TLP as illustrated in Figure 4-3. The wave surface elevation [52] is given by

$$rj(x,t) = \sqrt{2}\,\hat{}\sum_{\ddot{y}=i}^{N} y/S\hat{}\overline{(uJi)A(jj\ X}\ cos(KiX - w.t - <Pi) \qquad (6-1)$$

where

$u_{;,} = iAu$

Ki = wave nimaber

$(Pi$ = random phase angle uniformly distributed between 0 to 27r

N = a positive integer number.

Wave particle velocities and accelerations are simulated by using linear wave theory. The horizontal component $v(x\hat{}t)$ of the wave particle velocity at mean water level for a random wave with the modified JONSWAP spectrum $S_{,,}$ is expressed as

$$v(x,t) = V2\bar{\hat{}}\sum_{\dot{} = 1}^{N} V\hat{}n\ \overline{(wOAw\ X}\ 0JiCos(KiX - Uit + (pi), \qquad (6-2)$$

The horizontal component a(x, *t)* of the wave particle acceleration is obtained by differentiating Equation (6-4) with respect to time *t* as

$$a(x,t) = V2\bar{Y}I\ y/S\hat{}\overline{(ui)Au\ X}\ uj\hat{}sin(KiX - Uit - h <Pi), \qquad (6 - 3)$$

$$t = i$$

By using Equations (6-2) and (6-3), the wave particle velocity and the wave particle acceleration can be simulated at three different x-coordinates according to the location of the members (See Figure 4-3).

According to the modified Morison equation in Equation (4-2), the total force for the members is calculated by multiplying the force per unit length of columns and hulls with the submerged length of columns aind the effective length of hulls. The equation of motion for the TLP system can be written by the following:

$$m,\ddot{x} + Ax = F(x,t)$$

$$= \frac{1}{4} L[\hat{}pDCn(Uw\ '\hat{}Uc--\hat{})\backslash Uw\ +Uc--\hat{}\backslash \frac{dx}{dx}$$

$$-t'\hat{}piyUw \cdot \bullet t-'\hat{}pD'(Cm-l)Uw] \cdot \qquad (6-4)$$

where

L= length of the submerged column or effective length of the hull.

The nonlinearity of the equation of motion due to the square term of drag force can be solved using one of the step-by-step time integration methods, Newmark method [64], as the following:

$$\bar{\wedge}\wedge t+At = -Rt+At \qquad (6 — 5)$$

where

$$\bar{k} = m\wedge - \backslash - \frac{At\wedge}{T} \sim bk$$

$$Rt+At = \frac{At\wedge}{2} — bFt+\wedge t + m\,.\,[xt - tAtXt - \backslash - \frac{At\wedge}{2} — (l-b)xt]\wedge$$

The total force, $Ft+£,ti$ acting on structure at time, t -j- Ai, can be calculated from the right hand side of Equation (6-4). The coefficients used in Newmark method are o = 6 = J-,

By using the structure velocity and acceleration at time t, the structure response at time t -\- At can be calculated by Equation (6-4). The structure velocity and acceleration at time t -{• At can be obtained by the following equations:

$$\ddot{X}t+At = \frac{(1-b)}{\wedge} — \bar{X}t - \backslash - \wedge\wedge(\wedge * + A * - Xt - Atxt)^{2} \qquad (6 - 6)$$

$$\dot{X}t+\wedge t = it\text{-}t\ At[(l\text{-}a)xt\text{-}h\bar{a}xt+\wedge t]. \qquad (6\text{-}7)$$

Therefore, the structure response is simulated in time history. All response data can be statistically evaluated such as the mean response and the standard deviation response.

Briefly, the procedure of the superposition method for the time history of TLP response is summarized as the following steps:

1) Decompose the input wave height spectrum into the sufficient number of frequency.
2) Divide the whole frequency ranges into several blocks.
3) Simulate the wave particle velocity and the wave particle acceleration in time at each block.
4) By adding the wave particle velocity and the wave particle acceleration values at each time and dividing those values by the number of blocks, the averaged wave particle velocity and wave particle acceleration about the input wave height spectrum are simulated.
5) By using the wave particle velocity and acceleration simulation in time, calculate the wave and current force on the structure.
6) Solve the nonlinear equation of motion by using the step-by-step time integration method.
7) Find the structure response in time history.
8) Evaluate the statistical values such as the mean response and the standard deviation response of structure.

The work of this section is summarized in a computer flow chart in Figure 6-2.

6-4 Results and Discussion

The data for the random time-domain simulations are the following:

number of divisions = 7

number of frequencies = 401

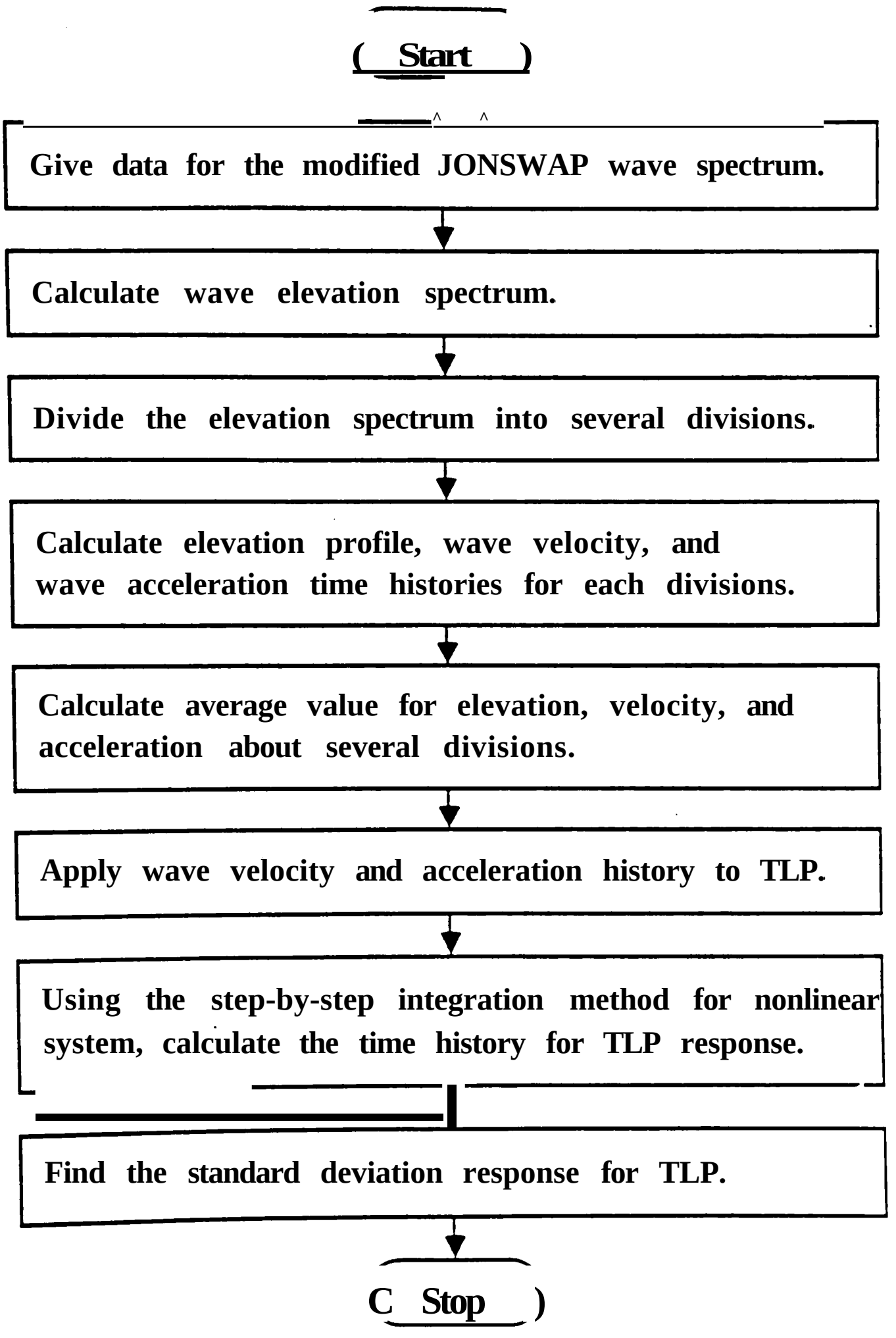

Figure 6-2 Flow chart for time-domain analysis

time step for step-by-step direct integration = 0.6 s.

The modified JONSWAP wave spectrum as shown in Figure 6-3 is used as the input wave energy spectrum. This figure is plotted with 401 frequencies. The simulated time histories of wave elevation, and wave acceleration at the horizontal center of the TLP are shown in Figures 6-4, 6-5, and 6-6. The numerical simulation is performed on IBM-3081 computer.

For surge response analysis, three different locations of a horizontal coordinate are considered because of different column locations of TLP model along the x direction. All velocity and acceleration simulations are simultaneously applied to the TLP. For solving the nonlinear dynamic equation, the step-by-step integration by the Newmark method was applied in every time step. The time history of the TLP response in the case of random wave only is shown in Figure 6-7. The time-domain analysis for random process with constant input is shown in Figures 6-8, 6-9, and 6-10, which displayed the shift of mean response.

To economize computation of time, a time average of one time history record is adopted in this simulation instead of a large number of response records. But the computation of time of one record is still about one hundred times greater than that of frequency-domain analysis in the case of random wave only. If many records are developed for more realistic phenomena and more accurate results, a great deal of computational time is involved.

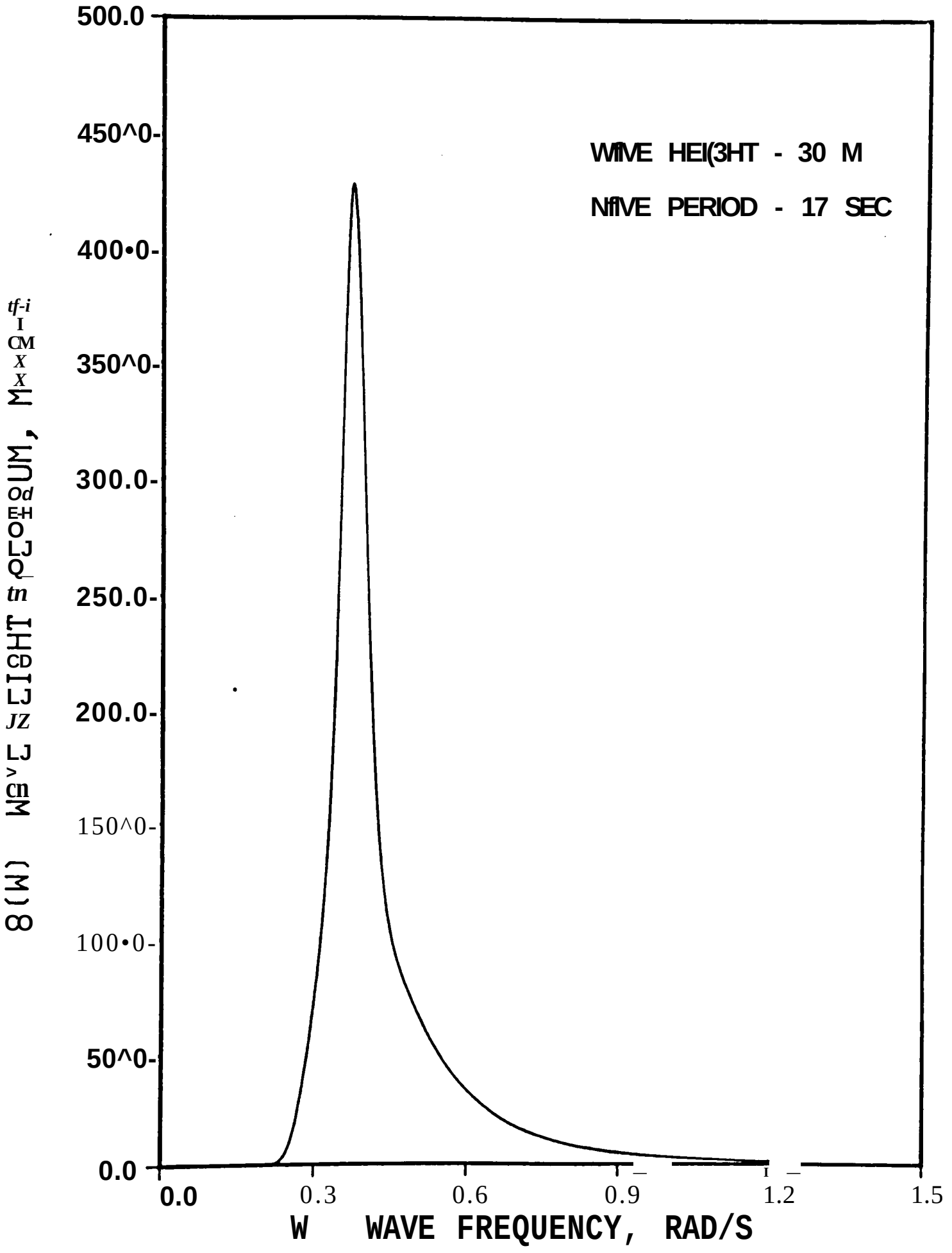

Figure 6-3 Modified JONSWAP wave spectrum with 401 wave frequencies

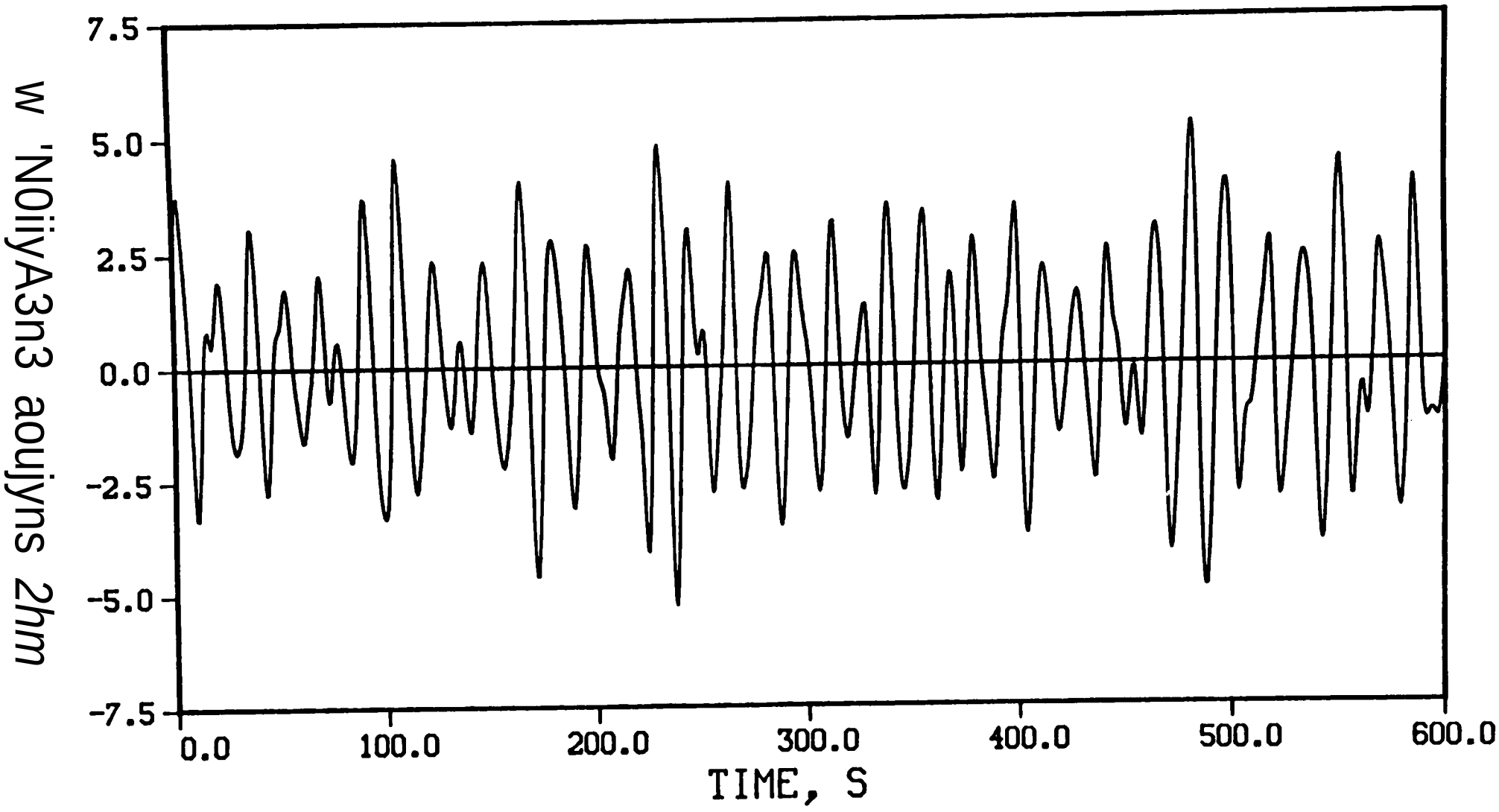

Figure 34 Wave height variation in time history

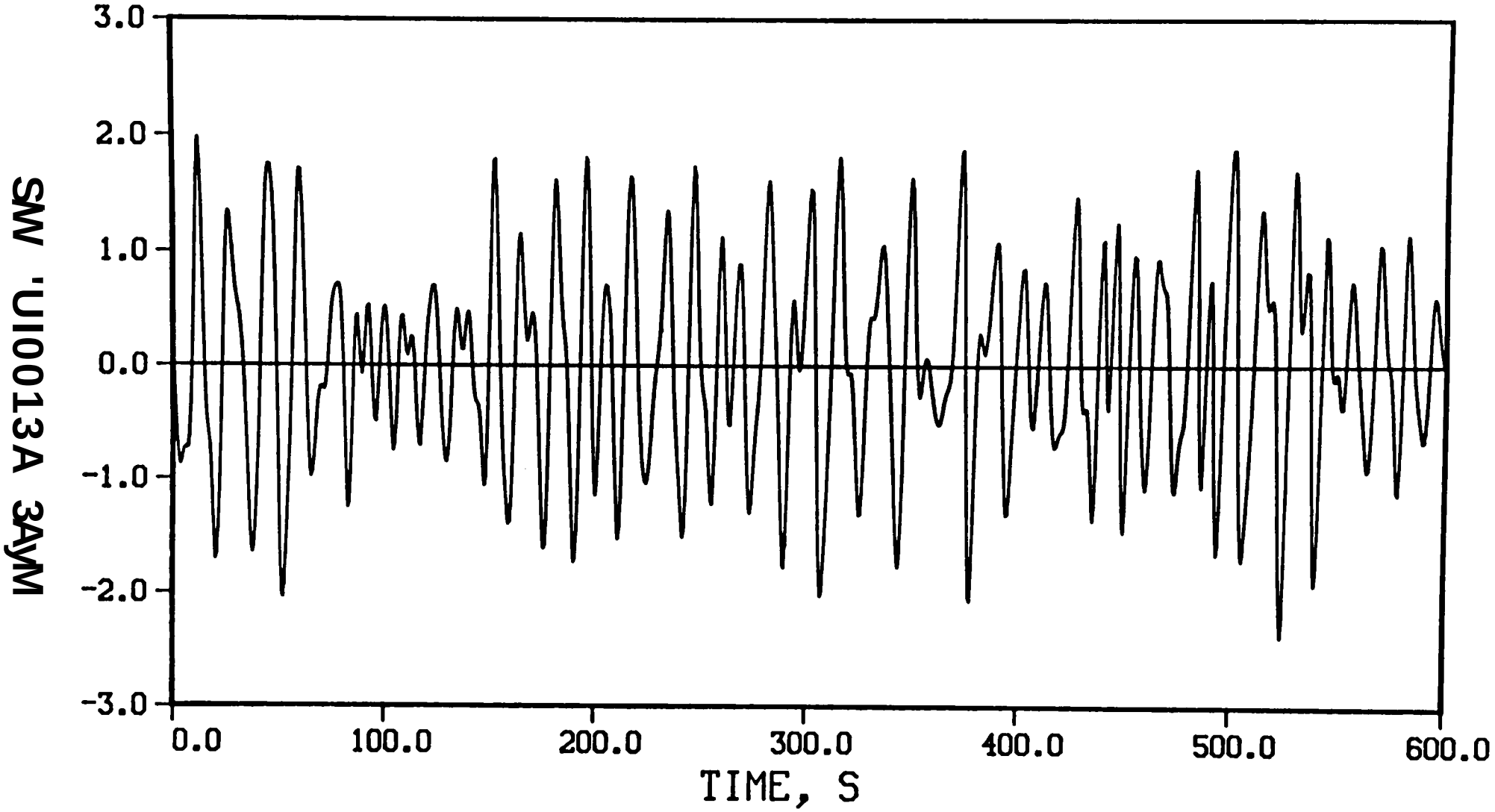

Figure 6-[illegible]e velocity[illegible]ulation in time history

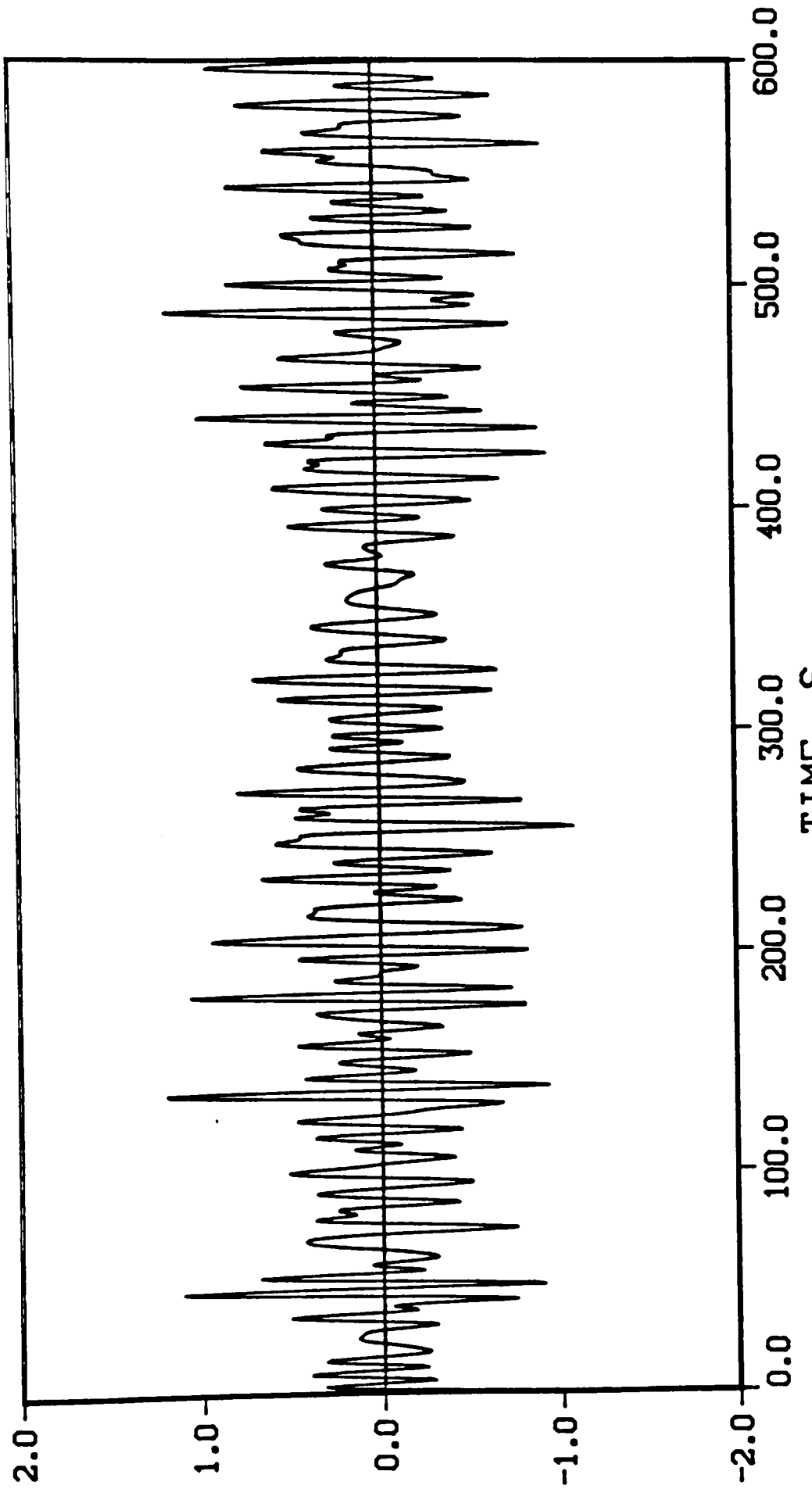

ZK><S/W 'N0IiyM3'1300U 3AyM

Figure 06 Wav< acceleration in time hi[illegible]

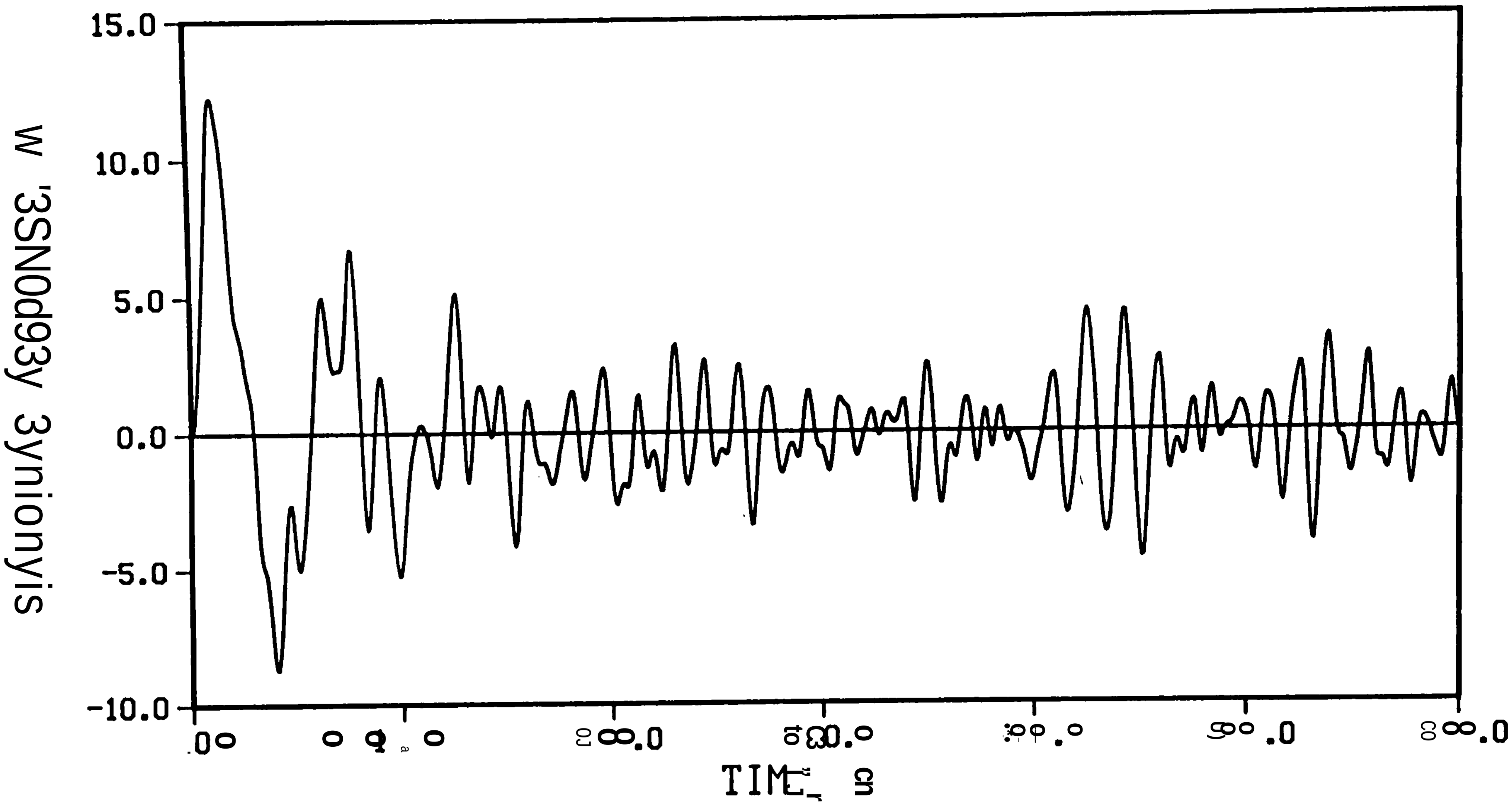

Figure 6-7 LP response history in the [illegible]

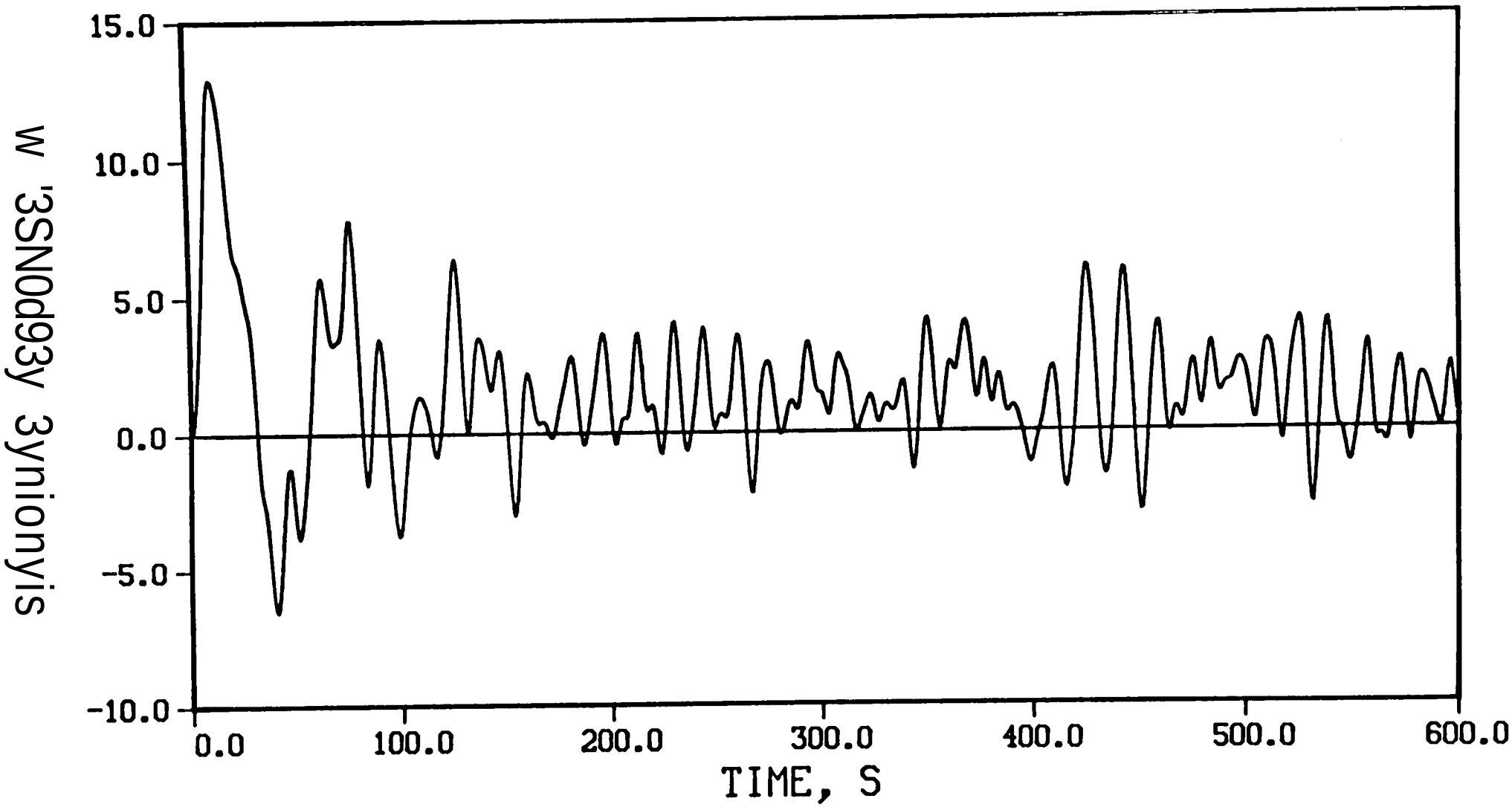

Figure 6-8 H[illegible]e history in mod[illegible] wave with current velocity, 1 knot

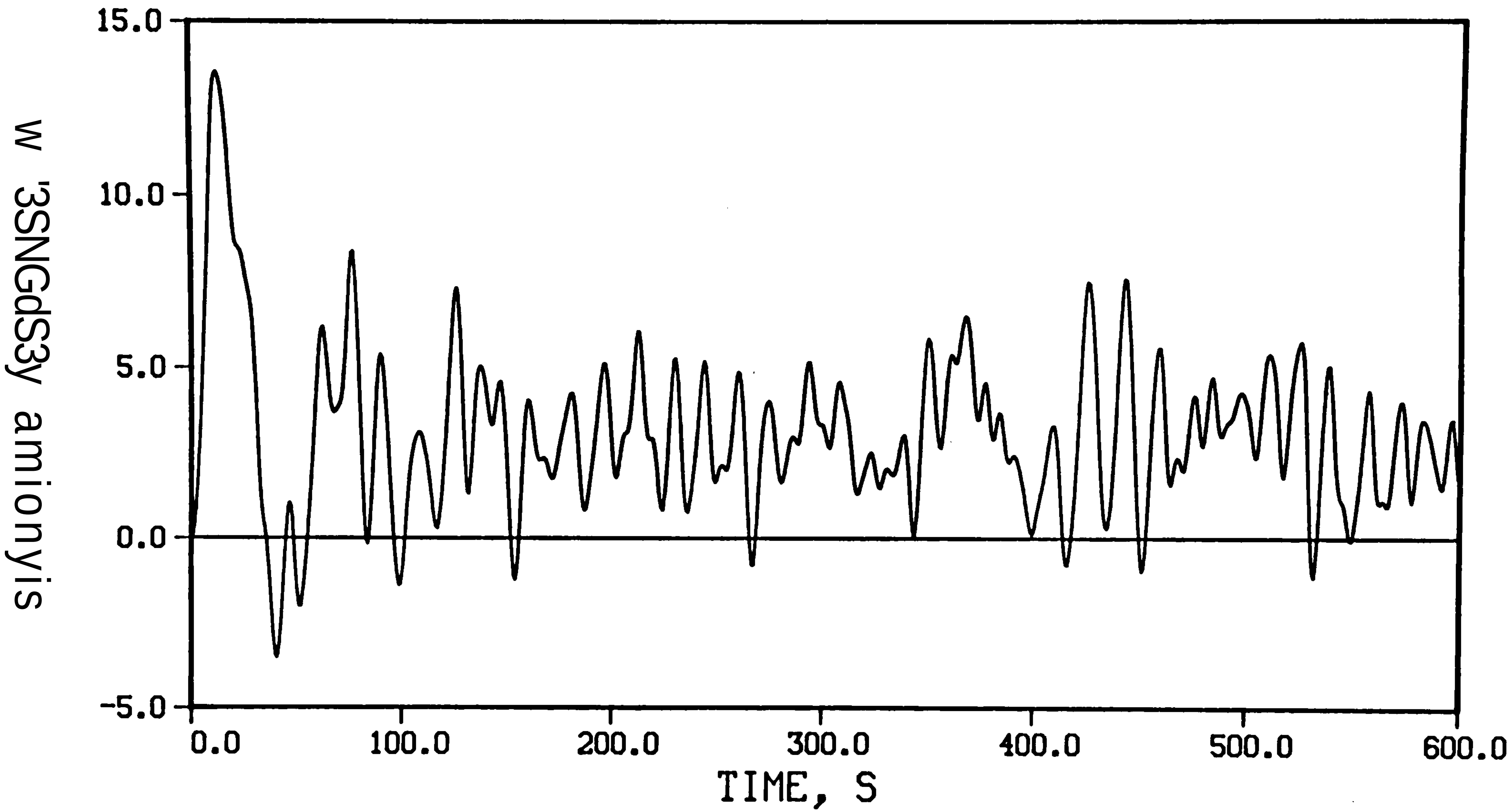

Figure 6-9 [illegible] response history in [illegible] with [illegible] velocity, 2 [illegible]

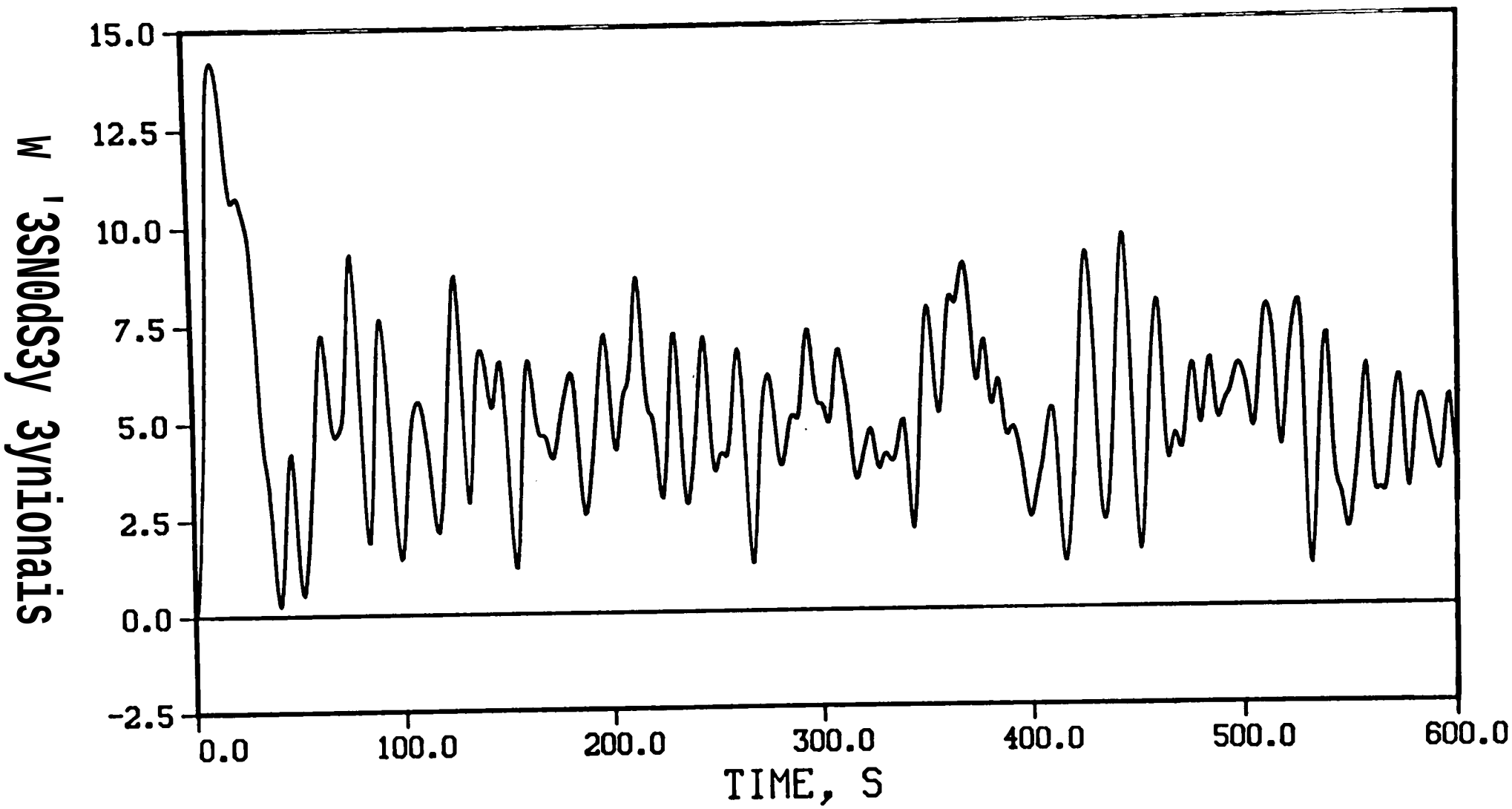

Figure 6[illegible] LP response history in rad s wave with c[illegible]t velocit[illegible] 3 k ot

The results of this research are shown in Table 6-1. In the case of random waves with current, the shift of mean value in time history can be explained by the effect of the constant current velocity. Therefore, the mean responses due to a steady current correspond to the static analysis due to current velocity in frequency-domain analysis.

The results change, depending on the time step, for the time step is very critical in time-domain analysis. Comparing the results of standard deviation responses in the frequency domain, the time-domain results with a time step of 0.6 s give a close value. The mean response of structure due to random wave only is close to zero.

6-5 Conclusions

The time-domain analysis for the dynamic analysis of offshore structure represents more realistic random phenomena, but it takes a lot of computational time. Also, depending on the size of record, the change of time step affects the results of statistical analysis. Therefore, it is important to choose the length of time record and the proper time step. With consideration of constant current velocity in time history analysis, the mean value of structure response is changed. The shift of mean value is the mean response due to current velocity.

Table 6-1 Results of surge response in time-domain analysis

		Standard deviation response (m)	Mean response (m)	Expected maximum response (m)	CPU time (sec)
Random wave only		2.588	0.094	13.293	175.22
Random wave with current profile	1 knot 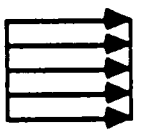	2.508	1.478	14.269	175.53
	2 knot 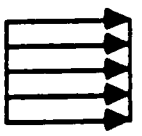	2.382	3.071	15.219	175.22
	3 knot 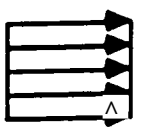	2.217	5.135	16.442	175.58

CHAPTER vn

DISCUSSION OF SOLUTIONS AND CONCLUSIONS

7-1 Comparison of Solutions

In this study, two consistent and effective TLP behavior solution techniques, namely frequency-domain and time-domain analysis, have been presented and compared for a specific problem. In the frequency-domain analysis, nonlinear drag force has been linearized by using an improved linearization technique. On the other hand, in the time-domain simulation, nonlinear drag force, which is proportional to the square of relative velocity due to water particle velocity and TLP structure velocity, has been taken into account.

For both numerical solution techniques the results are presented and compared in Table 7-1, In the case of random waves without current, time-domain and frequency-domain analysis show good agreement. From Table 7-1, the expected maximum response of TLP for the time domain analysis is 13.293 m with 175.22 s CPU solution time. On the other hand the frequency domain solution yields 13.403 m with 1.82 s CPU solution time. The frequency domain analysis for random waves without current shows considerable time saving in computational time (96 times less computational time). In the case of random waves with current does not agree well with the effect of constant current velocity. But, the expected maximum response

Table 7-1 Comparison of two analyses for surge motion

	Standard deviation response (m)		Mean response (m)		Expected maximum response (m)		CPU time (sec)	
	Freq. Dom.	Time Dom.	Freq. Dom.	Time Dom.	Freq. Dom.	Time Dom.	Freq. Dom.	Time Dom.
Random wave only	2.628	2.588	0.0	0.094	13.403	13.293	1.82	175.22
Current velocity 1 knot	2.527	2.508	3.254	1.478	16.142	14.269	5.71	175.53
Current velocity 2 knot	2.439	2.382	6.301	3.071	18.740	15.219	5.71	175.22
Current velocity 3 knot	2.361	2.217	9.296	5.135	21.337	16.442	5.71	175.58

for random wave with current velocity 1 knot has 13 percents difference between two analyses. Above this limit, the expected maximum responses for two methods are also widely different. From the results it can be seen that effect of the current velocity on the accuracy is significant. Obviously the difference must be involved with linearization of the drag term in the frequency domain analysis. Figure 7-1 shows the relation between linearization coefficients and current velocities. According to the adjustment of linearization coefficients, the mean response value in frequency-domain analysis can be close to the results of mean response of time domain. Therefore, the current velocity is a crucial factor in the dynamic analysis of offshore structures.

This comparison shows that for random waves without current, the frequency-domain analysis is very economical compared with the time-domain history analysis as far as computational time is is concerned. Also, the frequency-domain analysis with a new, improved linearization technique is recommended for the dynamic analysis of TLP's with random waves.

7-2 Final Conclusions

In order to model the TLP behavior accurately and economically, a suitable solution technique must be chosen. It may involve the time-domain or frequency-domain analysis. Through this research, the frequency-domain approach is recommended for the dynamic analysis of TLP with random waves. It is an economical and useful technique for the design of TLP's and

enables fairly rapid comprehensive parameter studies for each new application.

The main advantages of the linearized frequency-domain analysis are:

1. Considerable amount of saving on computer expense.

2. The solution converges fast (5-6 iterations).

The disadvantage of the linearized analysis is less accuracy due to linearization of the nonlinear hydrodynamic drag term. Therefore, it is important to choose new, improved linearization coefficients that depend on the application problems for the frequency-domain analysis.

Time-domain analysis needs to be considered as a worthwhile alternative for the design of TLP's. The main advantage of a time-domain analysis is accuracy. The disadvantage of a time-domain analysis is high cost of solution.

7-3 Recommendations

The recommendations for further study on the current research are as follows:

1, The linearization coefficients for TLP response analysis should be modified for high current velocity,

2, The influences of tether tension due to random waves only and the presence of current velocity should be studied.

3, Three-dimensional analysis of the TLP compared to the plane motion in the current research is needed for a more realistic computation.

4. A steady offset of the TLP can be considered.

5. Recent proposed techniques such as a Monte-Carlo simulation method and a time-series simulation method for time-domain analysis can be considered in the current study.

REFERENCES

1, Ellers, F,S.,"Advanced Offshore Oil Platforms," Scientiflc American, Vol. 246, April 1982, pp. 39-49,

2 Beynet, P,A. et al., "Motion, Fatigue, and the Reliability Characteristics of a Vertically Moored Platform," Offshore Technology Conference, Paper OTC 3304, 1978, pp. 2203-2212.

3. Spanos, P.D., and Agarwal, V.K., "Response of a Simple Tension Leg Platform Model to Wave Forces Calculated at Displaced Position," ASME Journal of Energy Resources Technology, Vol, 106, Dec. 1984, pp. 437-443,

4. Deleuil, G,E., Des Deserts, L,D., Doris, C.G., and Shive, A., "A New Method for Frequency Domain Analysis of Offshore Structures: Comparison with Time Domain Analysis," Offshore Technology Conference, Paper OTC 5303, 1986, pp. 103-110.

5. Yoneya, T., and Yoshida, K., "The Dynamic of Tension Leg Platforms in Waves," ASME Journal of Energy Resources Technology, Vol. 104, March 1982, pp. 20-28.

6. Albrecht, H.G., Koenig, D., and Kokkinowrachos, K., "Non-linear Dynamic Analysis of Tension Leg Platforms for Medium and Greater Depths," Offshore Technology Conference, Paper OTC 3044, 1978, pp. 7-15.

7. Denise, J-P. F,, and Heaf, N,J., "A Comparison between Linear and Non-linear Response of a Proposed Tension Leg Production Platform," Offshore Technology Conference, Paper OTC 3555, 1979, pp. 1743-1754.

8. Oran, C, "Overall Dynamic Characteristics of Tension Leg Platforms," Offshore Technology Conference, Paper OTC 4640, 1983, pp. 507-516.

9. Ninomiya, K,, Sawada, K., Katayama, M., and Unoki, K., "Non-linear Response Characteristics of TLP with and without Mechanical Damping System in Vary High Waves," Offshore Technology Conference, Paper OTC 4656, 1984.

10. Finnigan, T.D., Petrauskas, C, and Botelho, D.L.R., "Time Domain Model for TLP Surge Response in Extreme Sea States," Offshore Technology Conference, Paper OTC 4657, 1984, pp. 95-103.

11. Botelho, D.L.R., Finnigan, T.D., Petrauskas, C, and Liu, S.V., "Model Test Evaluation of a Frequency Domain Procedure for Extreme Surge Response Prediction of Tension Leg Platform," Offshore Technology Conference, Paper OTC 4658, 1984, pp. 105-112.

12. Yoshida, K., Ozaki, M,, and Oka, N,, "Structural Response Analysis of Tension Leg Platforms," ASME Journal of Energy Resource Technology, Vol, 106, March 1984, pp. 10-17.

13. Yashima, N., "The Experimental and Theoretical Study of a Tension Leg Platform in Deep Water," Offshore Technology Conference, Paper OTC 2690, 1976, pp. 849-856.

14. Paulling, J.R., and Horton, E.E., "Analysis of the Tension Leg Stable Platform," Offshore Technology Conference, Paper OTC 1263, 1970, pp. 379-390.

15. Sekia, K., and Sakai, M., "Modeling Tests To Establish a Design Method for TLP-Tether Systems," Offshore Technology Conference, Paper OTC 4653, 1984, pp. 51-57.

16. Jefferys, E.R., and Patel, M.H., "Dynamic Analysis Models of Tension Leg Platforms," ASME Journal of Energy Resources Technology, Vol, 104, September 1982, pp, 217-223,

17. Angelides, D.C., Chen, C-Y., and Will, S.A., "Dynamic Response of Tension Leg Platform," Proceedings of Boss, Vol, 2, 1982, pp. 100-122.

18. Kirk, C,L., and Jain, R,K,, "Wave Induced Oscillations of Tension-Leg Single Buoy Mooring System," Offshore Technology Conference, Paper OTC 2494, 1976, pp. 711-721,

19. Krolikowski, L,P,, and Gay, T.A., "An Improved Linearization Technique for Frequency Domain Riser Analysis," Offshore Technology Conference, Paper OTC 3777, 1980, pp. 341-353.

20. Ertas, A., and Kozik, T,J,, "Numerical Solution Techniques for Dynamic Analysis of Marine Riser," Journal of Energy Resource Technology,, Vol. 109, March 1987, pp. 1-5.

21. Ertas, A., "Linearization Technique for Probabilistic Riser Frequency Domain Analysis," Journal of Energy Resource Technology, Vol. 108, Dec. 1986, pp. 292-296.

22. Bernitsas, M.M., "Contributions Towards the Solution of Marine Riser Design Problem," Ph.D. Dissertation M.I.T., 1979.

23. Bernitsas, M.M., "On the Design of Marine Riser," Report to the American Bureau of Shipping, and Department of Naval Architecture and Marine Engineering, New England Section, The University of Michigan, May 1970.

24. Bernitsas, M.M., "A Three Dimensional Nonlinear, Large Deflection Model for Dynamic Behavior of Riser, Piplines and Cables," Journal of Ship Research, Vol. 26, March 1982, Number 1.

25. Leira, B.J., and Olufsen, A., "Biplanar Linearization of Drag Forces with Application to Riser Analysis," Offshore Technology Conference, Paper OTC 5100, 1986, pp. 167-181.

26. Wu, S.C, and Ray, J., "The Effects of Current on Dynamic Response of Offshore Platforms," Offshore Technology Conference, Paper OTC 2540, 1976, pp. 185-196.

27. Berge, B., and Penzien, J., "Three-Dimensional Stochastic Response of Offshore Towers to Wave Forces," Offshore Technology Conference, Paper OTC 2050, 1974, pp. 173-190.

28. Foster, E.T., "Model for Non-linear Dynamics of Offshore Structures," ASCE Journal of Engineering Mechanics, Vol. 96, 1970, pp. 41-67.

29. Langley, R.S., and Kirk, C.L., "Random Dynamic Analysis of an Offshore Single Anchor Leg Storage System," Applied Ocean Research, Vol. 4, 1982, pp. 232-236.

30. Langley, R.S,, "The Linearization of Three Dimensional Drag Force in Random Sea with Current," Applied Ocean Research, Vol. 6, 1984, pp. 126-131,

31. Malhotra, A.K,, and Penzien, J,, "Nondeterministic Analysis of Offshore Structures," ASCE Journal of Engineering Mechanics, Vol. 96, 1970, pp. 985-1003.

32. Sigbjornsson, R., and Smith, E,, "Wave Induced Vibrations of Gravity Platforms," Applied Mathematical Model, Vol. 4, 1980, pp, 155-165.

33. Spanos, D,P., "Linearization Technique for Non-linear Dynamic System," California Institute of Technology, Report EERL. 76-04.

34. Young, R.D,, Fowler, J.R., Fisher, E.A,, and Luke, R.R,, "Dynamic Analysis as an Aid to the Design of Marine Riser," ASME Energy Technology Conference and Exhibit, Pet-82, Texas, 1977, pp. 200-205.

35. Sarpkaya, T., and Isaacson, M., "Mechanic of Wave Forces on Offshore Structures," Van Nostrand Reinhold Co., New York, 1981.

36. Wilson, J.F, et al., "Dynamics of Offshore Structures," John Wiley <k Sons Co., New York, 1984,

37. Gaythwaite, J., "The Marine Environment and Structural Design," Van Nostrand Reinhold Co., New York, 1981.

38. Brebbia, C.A., and Walker, S., "Dynamic Analysis of Offshore Structures," Butterworth & Co., London, 1979.

39. Pierson, W.J., and Moskowitz, L., "A Proposed Spectral Form for Fully Developed Wind Seas Based on the Similarity Therory of S. A. Kitaigorodskii," Journal of Geophysical Research, Vol. 69, No. 24, 1964, pp. 5181-5190.

40. Hasselmann, K. et al,, "Measurements of Wind-wave Growth and Swell Decay During the Joint North Sea Wave Project," Erganzungsheft zur Deutschen Hydrographischen Zeitschrift, Reihe A (8), Nr, 12, 1973.

41. Hasselmann, K. et al., "A Parametric Wave Prediction Model," Journal of Physical Oceanography, Vol. 6, 1976, pp. 200-228.

42. Lee, W.T., and Bales, S.L., "A Modified JONSWAP Spectrum Development Only on Wave Height and Period," David W. Taylor Naval Ship Research and Development Center, Report No. SPD-0918-01, May 1980.

43. Longuet-Higgins, M.S., and Stewart, R.W., "The Changes in Amplitude of Short Gravity Waves on Steady Non-Uniform Currents," Journal of Fluid Mech., Vol. 10, 1961, pp. 529-549.

44. Huang, N,E,, Chen, D.T,, Tung, C C , and Smith, J.R,, "Interactions between Steady Nonuniform Currents and Gravity Waves with Applications for Current Measurements," Journal of Physical Oceanography, Vol. 2, 1972, pp, 420-431,

45. Tung, C.C., and Huang, N.E., "Influence of Current on Statistical Properties of Waves," Journal of the Waterways, Harbors and Coastal Eng. Divisions, ASCE Vol, 100, No, WW4, Nov, 1974, pp. 267-278.

46. Krylov, N., aind Bogoliubov, N., "Introduction to Nonlinear Mechanics," Princeton University Press, Princeton N.J., Annals of Mathematics Studies, Vol. 11, 1947.

47. Truxall, J. G., "Automatic Feedback Control System Synthesis," MacGraw Hill Company, New York, 1955.

48. Gelp, A., and Vander Velde, W.E., "Multiple-Input Describing Functions and Nonlinear System Design," McGraw-Hill Co., New York, 1968, pp. 370-396.

49. Chung, J.S., "Forced on Submerged Cylinders Oscillating Near a Free Surface," Journal of Hydronautics, Vol. 11, No. 3, July 1977, pp. 100-106.

50. Lee C.-K,, "Dynamic Response of Tension Leg Platform in a Random Sea]" Engineering Report, Texas A&M University, 1981.

51 Ochi, M.K., "On Prediction of Extreme Values," Journal of Ship Research. Vol? 17, No. 1, March 1973, pp. 23-27.

52. Borgman, L,E,, "Ocean Wave Simulation for Engineering Design," Journal of the Waterways and Harbors Division, ASCE Vol. 95, No. WW4, Proc. Paper 6925, Nov,,1969, pp, 557-583.

53. Burke, B.C., and Tighe, J.T,, "A Time Series Model for Dynamic Behavior of Offshore Structures," Offshore Technology Conference, Paper OTC 1403, 1971, pp, 775-788,

54. Godeau, A,J,, and Deleuil, G,E., "Dynamic Response and Fatigue Analysis of Fixed Offshore Structures," Offshore Technology Conference, Paper OTC 2260, 1975,

55. Godeau, A.J, et al,, "Statistical Analysis of Nonlinear Dynamic Response of Fixed Structures to Random Waves, Fatigue Evaluation," Offshore Technology Conference, Paper OTC 3030, 1977, pp. 493-502,

56. Hudspeth, R.T., "Wave Force Predictions from Nonlinear Random Sea Simulations," Offshore Technology Conference, Paper OTC 2193, 1975, pp. 471-480,

57. Hudspeth, R,T,, and Chen, M,-C,, "Digital Simulation of Nonlinear Random Waves," Journal of the Waterway Port Coastal and Ocean Division, ASCE Vol. 105, No. WWl, February 1979, pp. 67-85,

58. Hudspeth, R,T., and Borgman, L.E., "Efficient FFT Simulation of Digital Time Sequences," Journal of the Engineering Mechanics Division, ASCE Vol. 105, No. EM2, April 1979, pp. 223-235.

59. Shinozuka, M. et al., "Time-Domain Structural Response Simulation in a Shorted-Crested Sea," Journal of Energy Resources Technology, ASME Vol. 101, Dec. 1979, pp. 270-275.

60. Spanos, P-T.D., and Hansen, J.E., "Linear Prediction Theory for Digital Simulation of Sea Waves," Journal of Energy Resources Technology, ASME Vol. 103, September 1981, pp. 243-249.

61. Spanos, P-T.D., "ARMA Algorithms for Ocean Wave Modeling," ASME Journal of Energy Resources Technology, Vol. 105, September 1983, pp. 300-309.

62. Lin, N.K., and Hartt, W.H,, "Time Series Simulations of Wide-Band Spectra for Fatigue Tests of Offshore Structures," Journal of Energy Resources Technology, ASME Vol, 106, Dec. 1984, pp. 466-472.

63. Chakrabarti, S.K., "Seminar on Offshore Structure Hydrodynamics and Model Testing," Marine Research Division, CBI Industries INc, Plainfield, Illinois, June 2 - June 5, 1986.

64. Dhatt, G., and Touzot, G., "The Finite Element Method Displayed," John Wiley *k* Sons Inc., New York, 1984.

PERMISSION TO COPY

In presenting this thesis in partial fulfillment of the requirements for a master's degree at Texas Tech University, I agree that the Library and my major department shall make it freely available for research purposes. Permission to copy this thesis for scholarly purposes may be granted by the Director of the Library or my major professor. It is understood that any copying or publication of this thesis for financial gain shall not be allowed without my further written permission and that any user may be liable for copyright infringement.

Disagree (Permission not granted)	Agree (Permission granted)
_____	Jumbla Lee
Student's signature	Student's signature
_____	'Sys. i4, ms
Date	Date